Design and simulation of load adaptive energy saving schemes in IP over Wavelength-division multiplexing (WDM) networks

Asuquo, Asuquo Etim[1]
Department of Electrical and Electronic Engineering,
Akwa Ibom State University Mkpat Enin, Akwa Ibom State

Enyenihi Henry Johnson[2]
Department of Electrical and Electronic Engineering,
Akwa Ibom State University Mkpat Enin, Akwa Ibom State
enyenihijohnson@aksu.edu.ng

Ozuomba Simeon[3]
Department Of Electrical/Electronic And Computer Engineering,
University of Uyo, Akwa Ibom State Nigeria
simeonoz@yahoo.com
simeonozuomba@uniuyo.edu.ng

Abstract*— In this paper, Design and simulation of load adaptive energy saving schemes in IP over Wavelength-division multiplexing (WDM) networks is presented. This research seeks to use the Mixed Integer Linear Programming (MILP) technique to optimally reduce the total power consumption of an IP over WDM network with network coding implementation. This will be achieved by optimizing the routes each demand takes, and optimizing the number and location of conventional and network coding ports, for a given demand matrix and network topology. The architectural and mathematical models to realize energy consumption reduction in IP network-based applications and equipment over WDM networks are also presented. Simulation was conducted in MATLAB for performance evaluation of the models presented in this study. The analysis of the energy efficient IP over WDM network model was conducted for regular topologies, like ring, line, star and full mesh options, as well as for two real world core network, referred to as "SKYNET" and "ENIACNET. The SKYNET has 14 nodes and 21 links and an average hop count of 2.17, while the ENIACNET has 24 nodes and 43 links with an average hop count of 3. The traffic demand was evaluated using the average network traffic demand at various times of the day, according to a uniform distribution with values ranging from 20Gb/s to 120Gb/s. The MILP optimization was performed using the ANYLOGIC software running on a high performance computing cluster with 16 cores CPU and 256GB RAM. It is shown that by introducing network coding to SKYNET and ENIACNET topologies, daily average power savings of 27% and 33% are obtained respectively. Also, power savings asymptotically approach 45% and 22.5% for the ring (and line), and star topology respectively.

Keywords*— Energy Efficiency, Mixed Integer Linear Programming, Energy Saving Schemes, Wavelength-Division Multiplexing (WDM) Networks, Load Adaptive Scheme, Butterfly Network

1. Introduction

Over the last few decades, there has been unprecedented growth in network and Internet applications which has triggered demand for higher bandwidth and Quality of Service (QoS), as well as unparalleled diversification of network applications [1,2,3,4,5]. Similarly, innovations and developments in IP over Wavelength Division Multiplexing (WDM) networking technologies are focused basically on providing cheap and high-bandwidth transmission systems (up to 100 Gbps and beyond), flexible capacity utilization in IP-based technology, as well as layer-2 technologies and control and management solutions for dynamic provisioning of services [6,7,8,9,10,11,12,13,14] . However, while networking technologies are developing to satisfy the growing communication needs of the teeming user population across the globe, the attendant growth in energy demand of network infrastructures has become another concern, especially in this era of demand for green technologies [15,16,17,18,19].

According to studies, the network equipment of Information and Communication Technology (ICT) consumes about 24 GW of power, which relates to over 1% of the global electricity consumption [20,21,22,23,24]. The depleting oil reserves have made the cost of energy to

increase worldwide [25,26,27,28]. Hence, generally, energy reduction is now an important subject and in particular, there has been a continuous concern regarding the power consumption of different network elements. Moreover, the global warming, energy costs, power consumption and heat dissipation in the communication systems and data center make energy efficiency the main focus in of this paper 29,30,31,32,33].

Accordingly, the aim of this study centers on energy consumption reduction in IP network-based applications and equipment over WDM networks. The study determined the energy per bit consumption of IP and Ethernet i.e. the routers and switches, develop energy saving models for IP over WDM and also develop adaptive routing scheme using Mixed Integer Linear Programming and network coding partitioning scheme for core communication network via IP over WDM . The essence of all the models are to optimize the energy efficiency in the IP over Wavelength Division Multiplexing (WDM) networking infrastructures.

2. Methodology

2.1 The modelling of the energy saving scheme in IP over Wavelength-Division Multiplexing (WDM) networks

The major focus of the research is the design and simulation of adaptive energy saving schemes in IP over Wavelength Division Multiplexing (WDM) networks. Generally, the implementation of the traditional routing schemes requires complex computation to evaluate and optimize the energy consumption parameters in WDM networks especially, when dynamic optical circuits are introduced. This complication is taken further when the complete IP traffic matrix is not known. Consequently, the deployment of loads in IP over WDM networks uses the end-to-end circuit strategy which is typically provisioned for special applications. This is achieved at the expense of very high bandwidth demands while capacity allocation for IP traffic and capacity remains static.

This research presents modification in node architecture to improve energy efficiency (increase energy saving) of IP over WDM networks under unicast conditions. To enhance the energy efficiency on the node architecture, mixed integer linear programming (MILP) technique is used. Network coding is facilitated for the unicast bidirectional flows between node pairs by the proposed architecture. The new architecture also transforms the node functionality from “store and forward” to “store, code and forward”, where the coding is performed with the flow from opposite directions. This can be achieved either at the optical layer or the IP layer.

The butterfly network shown in Figure 1 illustrates the abstraction of the concept of network coding. The illustration shows that two units of information, X, and Y, are multicasted to two receivers, $d2$ and $d1$, respectively, by the sources k and n. Tracing transmission flow in a link (m,u) will always lead to a gridlock operation if all links have a unit capacity. An alternative to doubling the link capacity in order to resolve the gridlock is to share the link capacity by the two flows; encoding the flows by an XOR operation in node m, and multicasting the encoded flow to $d1$ and $d2$ from node u as shown in Figure 1.

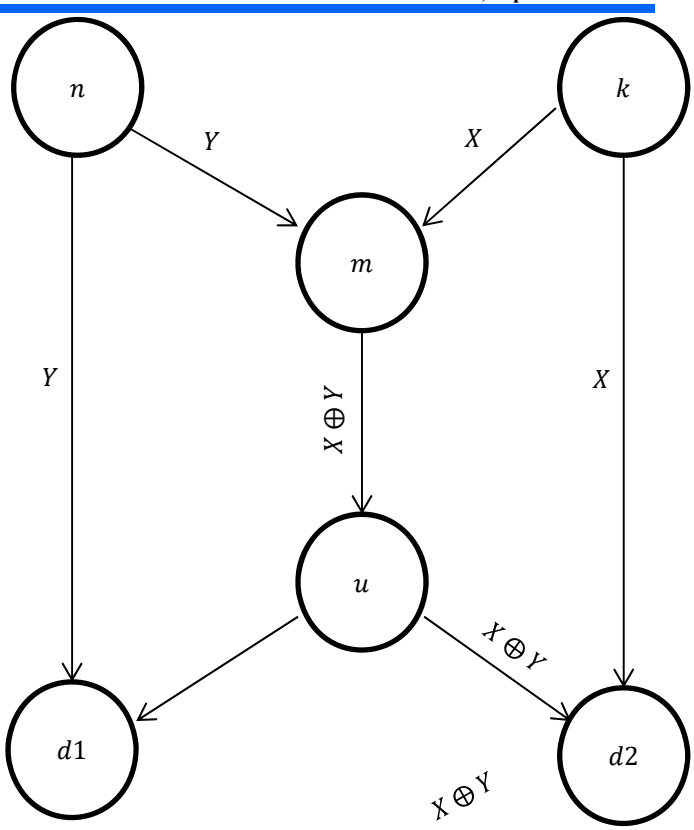

Figure 1 Schematic diagram of the butterfly network

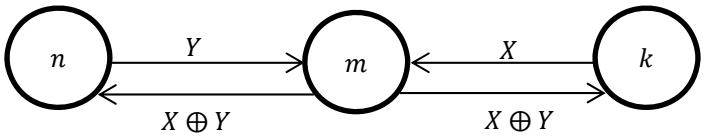

Figure 2 Schematic diagram of the three nodes network which is an exceptional case of the butterfly network.

An exceptional case of the butterfly network is presented in Figure 2 where each node pairs $(n,d1)$, (m,u), and $(k,d2)$ from Figure 1 are considered as a single node and the links connecting them are regarded as storage links rather than communication links. This configuration converts the butterfly network to a three node network, n, m, and k. It is certain that the special butterfly can carry out network coding in a unicast scenario. Assuming node k takes a fancy to send information units X to node n, and node n takes a fancy to send Y to node k, then both flows will be routed through the intermediate node m which can combine the flows using XOR gate and multicast back the encoded flow to both end nodes. At the receiving ends, each node retrieves the information units sent to it by XOR coding the received unit with the saved information unit. Resource saving is done at the middle node where coding is performed.

The proposed approach is further described in Figure 3a and Figure 3b. The modification in the node architecture is described in Figure 3b. The same ports as the conventional routing approach will be used at both the originating and terminating nodes. However, a single port that implements the coding functionality will substitute the two conventional ports at the intermediate nodes. Subsequently in this research, the term conventional port (architecture) will be used to refer to the current implementation while Network Coding (NC) (architecture) will be used to refer to the

network coding enabled IP port. The coding function in the context of this research work refers to modulo-2 addition (XOR). It is shown in Figure 3 that the number of ports on the three nodes is refactored from four conventional ports (Figure 3a) to one NC port and two conventional ports (Figure 3b). The quantity of power stored is the function of the ratio of the power consumed by the two types of ports and the network flow pattern.

The schematic diagram of the network coding node architecture is presented in Figure 4. In this case, an extra receiver is required, in addition to the transmitter and receiver found in the conventional ports. This addition is to enable the port to receive the two flows to be encoded. Storage is essential to synchronize data before encoding, because if synchronization in the IP layer is performed, different data flows will not reach the intermediate node at the same time.

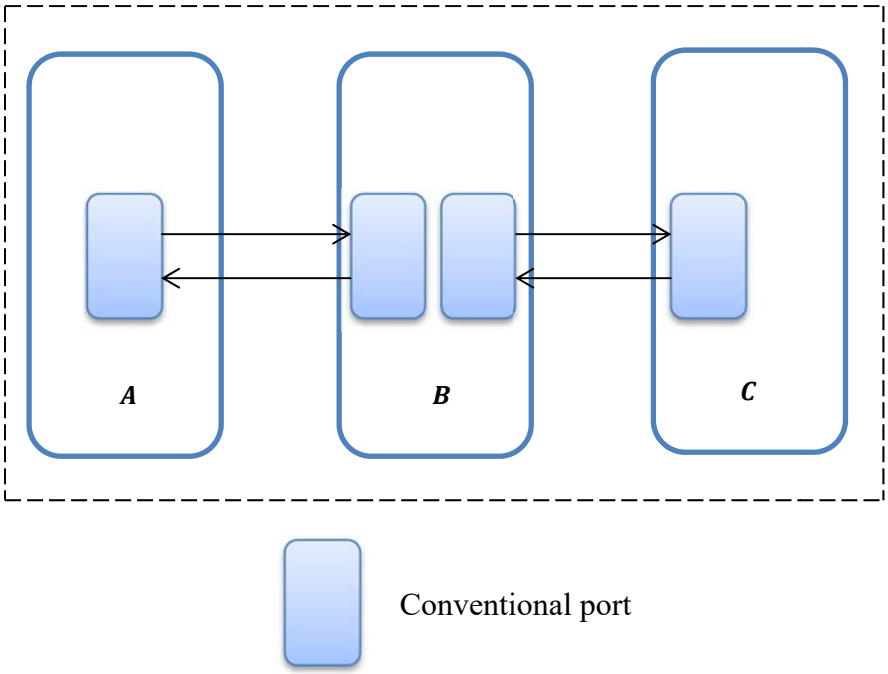

Figure 3 (a): Conventional port (architecture)

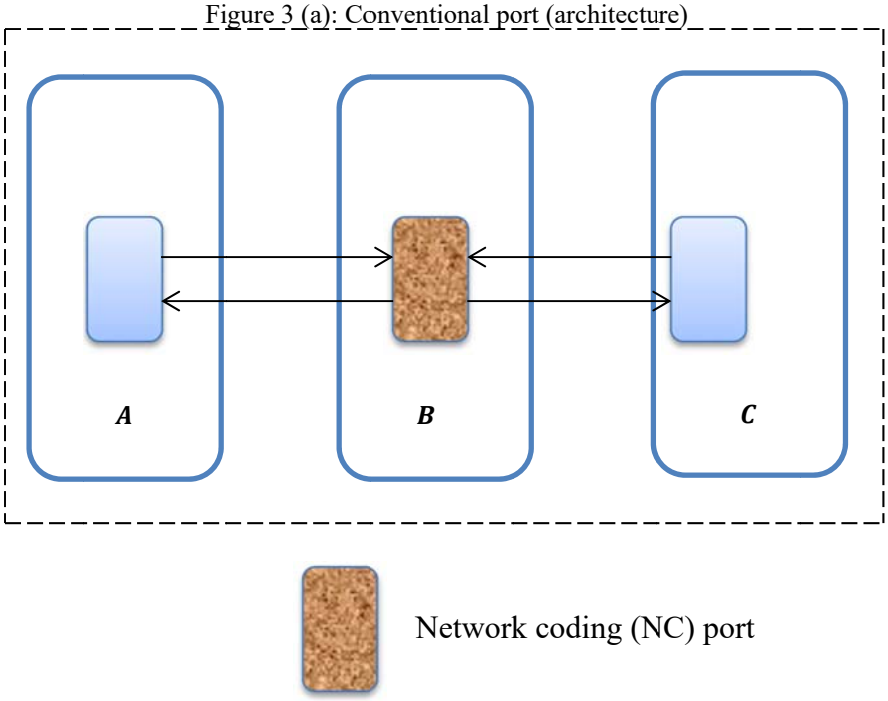

Figure 3 (b): Network coding (NC) (architecture)

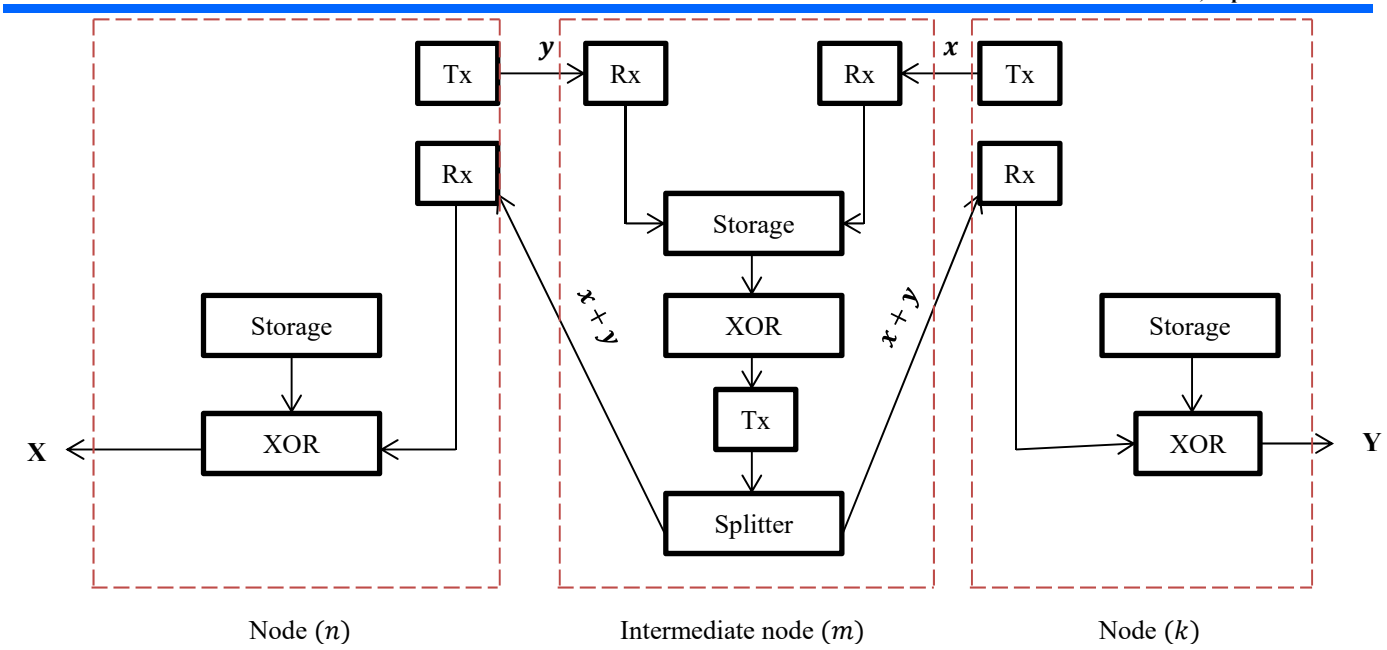

Figure 4 Network coding node architecture.

The flows encoding is performed by the XOR unit. In the optical layer, the transmitter is connected to a coupler and an amplifier which functions as multicast and compensator for power loss due to splitting. This approach supports long distance transmission effectively. The IP layer is where the coding operation is done, hence, the new coding scheme is implemented as an NC card which is plugged in the IP router chassis to support the conventional router cards. The storage unit is used to store the original information while the XOR decodes the received encoded flow; these happen on both the source and destination nodes. It should be noted that the storage functionality is already in existence in conventional ports; the XOR functionality is now part of processing and the coding is done on the IP layer which makes the additional storage and the XOR code come at a low cost. The IP implementation is more favorable to support this approach since all optical coding gates and controllable optical delay buffers are still in their early stage.

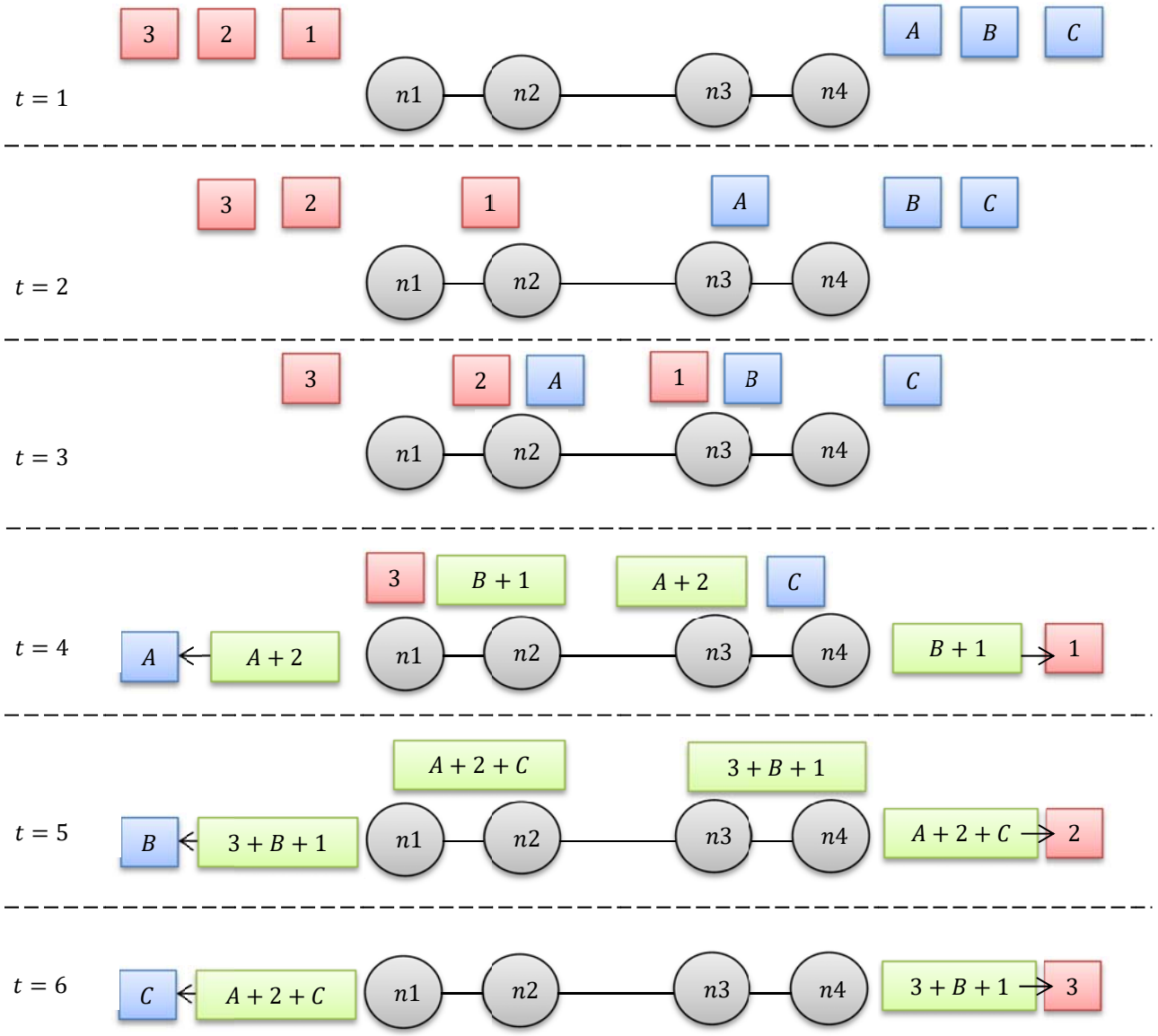

Figure 5 Network coding performed at two intermediate nodes.

Notably, in the node architecture, network coding can be carried out at all intermediate nodes of bidirectional flows. As shown in Figure 5, network coding is performed in a bidirectional flow, traversing two intermediate hops. Now, suppose node $n1$ transmits packets 1, 2, and 3 to node $n4$ while node $n4$ transmits packets A, B, and C to node $n1$. Note that the packets being transmitted, received or processed by a node are shown above the node as illustrated in Figure 5.

- At $t = 1$, $(n1)$ and $(n4)$ prepare packets (1) and (A), respectively for transmission.
- At $t = 2$, $(n1)$ and $(n4)$ prepare packets (2) and (B), respectively for transmission while packets (1) and (A) arrive at their neighboring intermediate nodes. No coding takes place at this point since the intermediate nodes receives only a single packet. The received packets are forwarded to the next node.
- At $t = 3$, Node $(n2)$ and $(n3)$ encode their packets to yield $(2 + A)$ and $(1 + B)$, respectively, while packets (1) and (B) arrive at node $(n3)$ and packets (2) and (A) arrive at node $(n2)$. At this point, the encoded packets are multicast to the neighboring nodes.
- At $t = 4$, $(n1)$ uses the stored packet (2) to decode the received packet $(A + 2)$. Similarly, $(n4)$ uses the stored packet (B) to decode the received packet $(B + 1)$. At this point, the intermediate nodes $(n2)$ and $(n3)$ has receive packets $(B + 1)$ and $(A + 2)$. These packets are decoded using the stored packets (1) and (A), to yield packets (B) and (2). Node $(n2)$ encodes (B) with (3) to yield $(B + 3)$, and $(n3)$ encodes (C) with (2) to yield $(C + 2)$, which are multicast simultaneously to their respective neighbors.
- At $t > 4$, the end nodes use their stored packets to decodes the received coded packets.

Packets synchronization is fully performed at reception and buffering is used to enhance the process. The decision of packets encoding in a given packet for metadata which is carried in the header is taken by the receiving nodes. The header information is negligible compared to the packet sizes. An additional chance is to perform coding on established path in a circuit switch network; decisions on paths taken and coding possibilities decided too, on time. It

is assumed in this research that the management and control overhead is negligible since it can be carried out as a result of system software upgrade.

3.2 The mixed integer linear programming model for optimizing the energy saving scheme

This research seeks to use the Mixed Integer Linear Programming (MILP) technique to optimally reduce the total power consumption of a non-bypass IP over WDM network with previously mentioned network coding implementation. This will be achieved by optimizing the routes each demand takes, and optimizing the number and location of conventional and NC ports, for a given demand matrix and network topology.

It is assumed that the network is totally synchronized, which means that the information units to be XOR coded are buffered before being coded and they arrive at the same time. The randomness of the arrival process determines the requirement for buffering. The delay introduced by XOR coding process is damped by the buffering process. It is apposite to note that the upshot of this assumption is the introduction of a lower bound on power consumption. In real-time communication requirements, the coding process could be forced to encode only traffic with stream of zero, thereby minimizing the potential of network coding with respect to energy. The total power consumption is defined as;

$$P_T = \sum_{m\in N}\left(P_p Y_m + P_x X_m + Po_m + Pmd_m + \sum_{n\in N_m}(P_t w_{mn} + P_e A_{mn} f_{mn})\right) \quad (1)$$

Where P_T = total power consumption of the network (W), P_p = power consumption of a conventional router port, Y_m = number of conventional ports at node m, P_x = power consumption of NC router port, X_m = number of NC ports at node m, Po = power consumption of and optical switch, Pmd = power consumption of a multiplexer/de-multiplexer, P_t = power consumption of a transponder, w_{mn} = total traffic flow carried on physical link, P_e = power consumption of erbium-doped fiber amplifier (EDFA), A_{mn} = the number of EDFAs on physical link (m,n), f_{mn} = the number of fiber on physical link (m,n). The analytical expressions for the components of the total power consumption are hereby presented. Let the total power consumption of conventional router port is expressed as:

$$\sum_{m\in N}\left(P_p Y_m\right) \quad (2)$$

Let the total power consumption of NC router port is expressed as:

$$\sum_{m\in N}(P_x X_m) \quad (3)$$

Let the total power consumption of optical switches is expressed as:

$$\sum_{m\in N}(Po_m) \quad (4)$$

Let the total power consumption contribution from multiplexers and de-multiplexers be expressed as:

$$\sum_{m\in N}(Pmd_m) \quad (5)$$

Let the total power consumption of transponders be expressed as:

$$\sum_{m\in N}\sum_{n\in N_m}(P_t w_{mn}) \quad (6)$$

And the power consumption of all the EDFAs be expressed as:

$$\sum_{m\in N}\sum_{n\in N_m}(P_e A_{mn} f_{mn}) \quad (7)$$

Subject to:

$$\sum_{n\in N_m} b_{mn}^{sd} - \sum_{n\in N_m} b_{nm}^{sd} = \begin{cases} 1 : & m = s \\ -1 : & m = d \\ 0 : & otherwise \end{cases} \quad (8)$$
$$\forall s,d,m \in N$$

Where $b_{m,n}^{sd}$ is the binary equivalent of $w_{m,n}^{sd}$. $b_{m,n}^{sd} = 1$, if $w_{m,n}^{sd} > 0$, $b_{m,n}^{sd} = 0$ otherwise. $w_{m,n}^{sd}$ is the traffic flow between node pair (s,d) that traverses the physical link (m,n) in Gbps.

The constraint in Equation 8 denotes the flow conservation constraint where the total incoming traffic equates the outgoing traffic for all nodes apart from the source and destination nodes. The flow of traffic demand that traverses a link based on the binary variable b_{mn}^{sd} can be calculated by the constraint defined as;

$$w_{mn}^{sd} = \lambda^{sd} b_{mn}^{sd} \quad (9)$$
$$\forall s,d \in N, \forall m \in N, n \in N_m$$

Where λ^{sd} is the volume of demand (s,d) in multiples of wavelength. The total traffic on a given link which is denoted by the total flow of all demands passing through that link is expressed as:

$$w_{mn} = \sum_{s\in N}\sum_{d\in N: s\neq d} w_{mn}^{sd} \quad (10)$$
$$\forall m \in N, n \in N_m$$

In order to ensure the link capacity conservation, the constraint in Equation 10 is applied. The total flow on a link must not exceed the total capacity of al fiber on that link.

$$\sum_{s\in N}\sum_{d\in N: s\neq d} w_{mn}^{sd} \leq W B f_{mn} \quad (11)$$

Where B is the wavelength capacity. The MILP model will be relaxed for now, hence, Equation 12 and Equation 13 will be used for the MILP implementation instead of the more accurate $\left\lceil \sum_{s\in N}\sum_{\substack{d\in N \\ s\neq d \\ s=m}} \frac{w_{mn}^{sd}}{B} \right\rceil$ and $\left\lceil \sum_{s\in N}\sum_{\substack{d\in N \\ s\neq d \\ d=m}} \frac{w_{mn}^{sd}}{B} \right\rceil$, respectively, which select the next integer greater than the real value.

$$Npo_{mn} = \sum_{s\in N}\sum_{\substack{d\in N \\ s\neq d \\ s=m}} \frac{w_{mn}^{sd}}{B} \quad (12)$$

$$Npi_{mn} = \sum_{s\in N}\sum_{\substack{d\in N \\ s\neq d \\ d=m}} \frac{w_{mn}^{sd}}{B} \quad (13)$$

At this point, the number of ports leaving and entering a node is governed by Equation 3.10 and Equation 13 respectively. It should be noted that router ports have a pair (Tx and Rx) components; and under asymmetric traffic condition, the number of ports required is determined by the largest between the outgoing and incoming traffic which is determined as:

$$Np_{mn} = \max(Npo_{mn}, Npi_{mn}) \quad (14)$$
$$\forall m \in N, n \in N_m$$

Then, the total number of conventional ports is given by:

$$Y_m = \sum_{n\in N_m} Np_{mn} \quad (15)$$
$$\forall m \in N$$

$$c_{nmk}^{sd} \leq b_{nm}^{sd} \quad (16)$$

$$c_{nmk}^{sd} \leq b_{mk}^{sd} \quad (17)$$

$$c_{nmk}^{sd} \geq b_{nm}^{sd} + b_{mk}^{sd} - 1 \quad (18)$$
$$\forall s,d \in N, \forall m,n,k \in N : m \neq n \neq k$$

Where $c_{nmk}^{sd} = 1$ if demand (s,d) traverses link (n,m) and (m,k), which means that bidirectional traffic flows can be encoded in node m.

The variable c_{nmk}^{sd} is computed by Equation 16, Equation 3.17, and Equation 18 for each node and different flows. The three constraints presented are equivalent to $c_{nmk}^{sd} = b_{nm}^{sd} b_{mk}^{sd}$, which are used to sustain the model linearity that is otherwise lost due to variable multiplication. The total number of coded ports at node m that encodes the bidirectional traffic between node pair (n,k) is computed by the constraint given as ;

$$X_{nk}^{m} = \sum_{s\in N} \sum_{\substack{d\in N \\ s\neq d}} \max\left(\frac{c_{nmk}^{sd}\lambda^{sd}, c_{nmk}^{ds}\lambda^{ds}}{B}\right), \quad (19)$$
$$\forall m,n,k \in N : m \neq n \neq k$$

It should be noted that the number of NC ports at any given node is determined based on the maximum flow of the directional traffic demand of which the node is intermediate. The non-linearity of the model is defined by the introduction of the max() function in Equation 19. To compute the traffic flow value from node n to node k, passing through node m, the following expression is used.

$$w_{nk}^{m} = \sum_{s\in N} \sum_{\substack{d\in N \\ s\neq d}} c_{nmk}^{sd}\lambda^{sd} \quad (20)$$

The variable Δ_{nk}^{m+} is introduced as binary variable, to determine the maximum directional flows between w_{nk}^{m} and w_{kn}^{m}. This also helps in informing about the difference of flow polarity (positive or negative). The difference of bidirectional traffic between nodes n,k that passes through node m, is computed by the variable Δ_{nk}^{m} as given as;

$$\Delta_{nk}^{m} = w_{nk}^{m} - w_{kn}^{m} \quad (21)$$
$$\forall m,n,k \in N : m \neq n \neq k$$

$$\Delta_{nk}^{m} \leq M\Delta_{nk}^{m+} \quad (22)$$
$$\Delta_{nk}^{m} \geq -M\Delta_{nk}^{m-} \quad (23)$$

The polarity of the bidirectional flow difference variable is indicated by the binary indicator variables Δ_{nk}^{m+} and Δ_{nk}^{m-}. If the flow difference variable (Δ_{nk}^{m}) is positive, $\Delta_{nk}^{m+} = 1$, and if (Δ_{nk}^{m}) is negative, $\Delta_{nk}^{m-} = 1$. The instance of $(\Delta_{nk}^{m} = 0)$ implies that both Δ_{nk}^{m+} and Δ_{nk}^{m-} can have the value 0 or 1. Relevant constraint must be applied to ensure that the two variables are not both set to 1, hence, to resolve the ambiguity the constraint in following expression must be satisfied.

$$\Delta_{nk}^{m+} + \Delta_{nk}^{m-} \leq 1 \quad (24)$$

$$X_{nk}^{m} = \begin{cases} \frac{w_{nk}^{m}}{B} & if\ \Delta_{nk}^{m+} = 1 \\ \frac{w_{kn}^{m}}{B} & otherwise \end{cases} \quad \forall m,s,d \in N, n,k \in N_m, n < k \quad (25)$$

Then, the total number of NC ports at each node is computed using the expression;

$$X_m = \sum_{n\in N_m} \sum_{\substack{k\in N_m \\ n<k}} X_{nk}^{m} \quad (26)$$

2.3 Network Coding with Partitioning

In section 2.2, it was assumed that the smaller of the two bidirectional flows is padded with zeros before encoding it, which makes the higher of the two bidirectional flows to be used to compute the resources used. This section presents an alternative approach to prepare packets for network coding. This approach involves partitioning the bigger packet into two parts; while the first part has the size of the smaller packet, the remaining part is routed without encoding. The zero padding and the partitioning approach are presented in Figure 6a and Figure 6b, respectively.

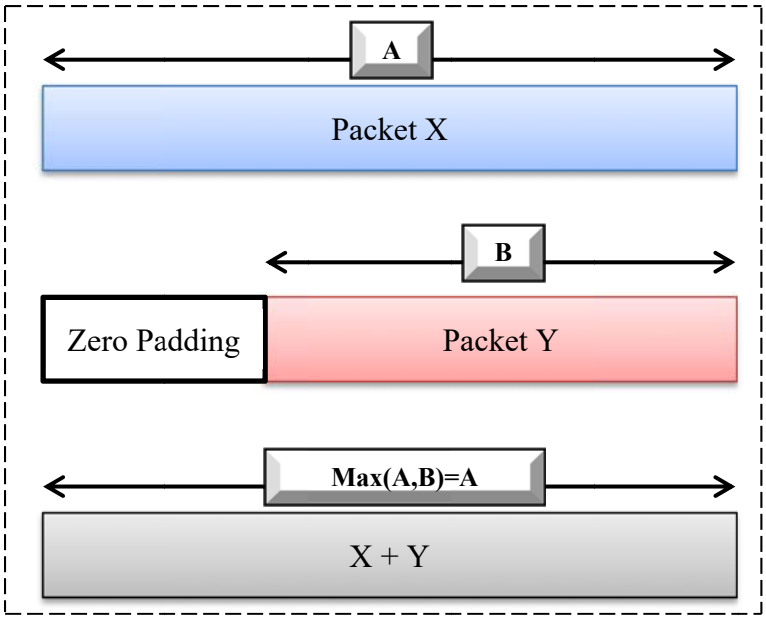

Figure 6 (a): Network coding with zero padding

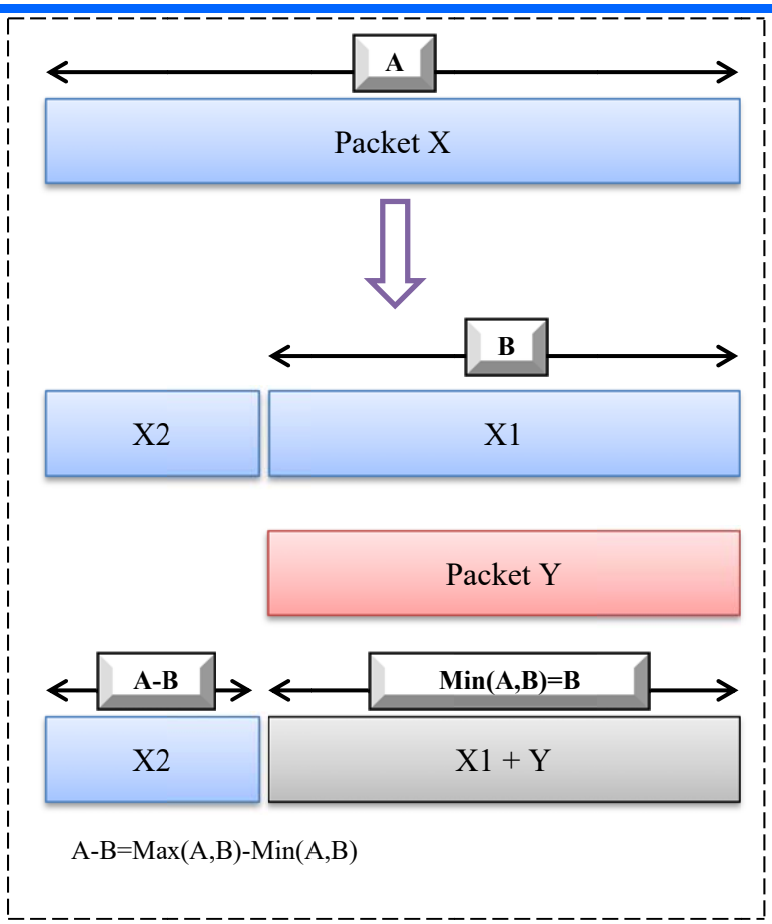

Figure 6(b): Network coding with partitioning

The zero padding method appears to be the simpler approach; however, it has less resource efficiency. Conversely, the partitioning method conserves resources at the cost of adding management and control overhead to decide how and when to segment packets for maximum benefit. Having this in mind, the variable Y_{nk}^{m} will be updated to represent the difference between the two packet size and is calculated as:

$$Y_{nk}^{m} = \frac{w_{nk}^{m} - w_{kn}^{m}}{B} \quad (27)$$

Thus, changing the variable X_{nk}^{m} to denote the minimum of the opposite flows which will influence Equation 19 to change to:

$$X_{nk}^{m} = \sum_{s\in N}\sum_{\substack{d\in N \\ s\neq d}} min\left(\frac{c_{nmk}^{sd}\lambda^{sd}, c_{nmk}^{ds}\lambda^{ds}}{B}\right) \quad (28)$$

Then, Equation 25 will be change to:

$$X_{nk}^{m} = \begin{cases} \frac{w_{nk}^{m}}{B} & if\ \Delta_{nk}^{m-} = 1 \\ \frac{w_{kn}^{m}}{B} & otherwise \end{cases} \quad (29)$$

The total number of conventional port is then calculated as:

$$Y_{m} = \sum_{n\in N_m}\sum_{s\in N}\sum_{\substack{d\in N \\ s\neq d}} \frac{w_{nm}^{sd}}{B} + \sum_{n\in N_m}\sum_{k\in N_m} Y_{nk}^{m} \quad (30)$$

The number of conventional ports with zero padding case is produced by the first term of Equation 30, where the zero padding case utilized the max() function as shown in Equation 3.12. Since the traffic was asymmetric, the use of max() function was necessary. The second term of Equation 30 accounts for the residual flow from the partitioning process.

2.4 Bounds on "Energy Efficient" Network Coding

This section focuses on deriving closed form expressions and analytical bounds for the power consumption of networks that implements network coding. The bounds for network coding with partitioning as well as zero padding are considered in this analysis.

3.4.1 Conventional Scenario

Consider $G(N, E)$ as a network which comprises of a collection of undirected edges, E, connecting a set of nodes, N. Let the bidirectional traffic demand be defined as the tripartite (s, d, λ^{sd}), where $s \in N$ and $d \in N$ represents the end nodes of the demand and λ^{sd} represents the data rate requirement of the demand. Supposing each demand proceeds on a single path, then the hop count traversed by a single traffic flow of the bidirectional demand is given by:

$$h^{sd} = \sum_{m\in N}\sum_{n\in N_m} b_{mn}^{sd} \quad (31)$$

Where b_{mn}^{sd} is a binary variable and it equals to 1 if the flow between the node pair (s, d) is routed through the link (m, n), and equals to 0 otherwise. Then the network average hop count for all flows is given as:

$$h = \frac{1}{N(N-1)}\sum_{s\in N}\sum_{\substack{d\in N \\ s\neq d}} h^{sd} \quad (32)$$

In a conventional IP over WDM network (under non-bypass approach), the power consumption of a single traffic flow (s, d), of a bidirectional demand is given by:

$$P_{sd} = (P_p + P_t)\sum_{m\in N}\sum_{n\in N_m} \frac{w_{mn}^{sd}}{B} \quad (33)$$

This research considers only the most power consuming devices, such as router ports, and transponders, for simplicity. The integration of traffic grooming yields efficient wavelength and improves accuracy. Suppose all

the network demands are equal, which means that $\lambda^{sd} = \lambda$ $\forall s, d \in N, s \neq d$, then,

$$\sum_{m\in N}\sum_{n\in N_m} w_{mn}^{sd} = \lambda \sum_{m\in N}\sum_{n\in N_m} b_{m,n}^{sd} = \lambda h^{sd} \quad (34)$$

This implies that the power consumption of a single flow can be represented as;

$$P_{sd} = \left(\frac{P_p + P_t}{B}\right)\lambda h^{sd} \quad (35)$$

Then, the overall network power consumption can be expressed as:

$$P = \left(\frac{P_p + P_t}{B}\right)\lambda \sum_{s\in N}\sum_{\substack{d\in N \\ s\neq d}} h^{sd} \quad (36)$$

Let $P_\lambda^{sd} = \left(\frac{P_p + P_t}{B}\right)$, and λ^{sd} represents a single hop power consumption and $P_\lambda^{sd} = P_\lambda$, $\forall s, d \in N, s \neq d$, then the power consumption can be expressed as:

$$P = P_\lambda \sum_{s\in N}\sum_{\substack{d\in N \\ s\neq d}} h^{sd} \quad (37)$$

Therefore, the hop count of the network traffic demand can be expressed as a function of the overall hop count h which is expressed as;

$$\sum_{s\in N}\sum_{\substack{d\in N \\ s\neq d}} h^{sd} = N(N-1)\frac{\sum_s\sum_d h^{sd}}{N(N-1)} = N(N-1)h \quad (38)$$

Then, power consumption of IP over WDM network can be expressed as:

$$P = P_\lambda hN(N-1) \quad (39)$$

2.4.2 Network Coding Scenario

For IP over WDM network implemented with network coding, both flows of the bidirectional demands are routed through the same path, which is the reason network coding is performed at the intermediate nodes. The implication in this case is that the power consumption of both flows of the bidirectional demand (s, d) and (d, s) is expressed as:

$$\widetilde{Psd} = 2\left(\frac{P_p + P_t}{B}\right)\lambda^{sd} + \left(\frac{P_p + P_x}{B}\right)\lambda^{sd}(h^{sd} - 1), \quad \forall s, d \in N, s < d \quad (40)$$

From Equation 40, the first term accounts for the power consumption of end nodes where a conventional port is used to send and receive the flows at each end. Since the power consumption of the XOR gate and storage at the end nodes are negligible, they are eliminated from this analysis. The second term is imputed due to the intermediate nodes where coding is carried out. Notice that Equation 40 is evaluated for all values of $s < d$ instead of $s \neq d$. $\widetilde{Psd}$ computes the total power consumed for the flow (s, d) and (d, s). Hence, the power consumption can be rearranged and expressed as:

$$\widetilde{Psd} = 2\lambda^{sd}\frac{P_p + P_t}{B}\left(1 + \frac{P_t + P_x}{P_p + P_t}\left(\frac{h^{sd}-1}{2}\right)\right) \quad (41)$$

If $r = \frac{P_t + P_x}{P_p + P_t}$, and denotes the ration of power consumption of the network coding scheme, and the conventional scheme, then the power consumption of the bidirectional demand can be expressed as:

$$\widetilde{Psd} = 2P_\lambda^{sd}\left(1 + r\frac{h^{sd}-1}{2}\right) \quad (42)$$

Hence, the network total power consumption, taking cognizance of network coding is expressed as:

$$\tilde{P} = 2\sum_{s\in N}\sum_{\substack{d\in N \\ d<s}}\left(P_\lambda^{sd} + P_\lambda^{sd} r\frac{h^{sd}-1}{2}\right) \quad (43)$$

Resulting in:

$$\tilde{P} = 2\left(\sum_{s\in N}\sum_{\substack{d\in N \\ d<s}} P_\lambda^{sd}\left(1 - \frac{r}{2}\right) + \frac{r}{2}\sum_{s\in N}\sum_{\substack{d\in N \\ d<s}} P_\lambda^{sd} h^{sd}\right) \quad (44)$$

If all demands in the network have equal value, meaning that $P_\lambda^{sd} = P_\lambda$, $\forall s, d \in N$, then the total power consumption becomes;

$$\tilde{P} = 2P_\lambda\left(\left(1 - \frac{r}{2}\right)\left(\frac{N(N-1)}{2}\right) + \frac{rN(N-1)h}{4}\right) \quad (45)$$

$$\tilde{P} = P_\lambda N(N-1)\left(1 + \frac{r}{2}(h-1)\right) \quad (46)$$

Let power savings be denoted by ϕ, then, ϕ is expressed as:

$$\phi = 1 - \frac{\tilde{P}}{P} = 1 - \left(\frac{P_\lambda N(N-1)\left(1 + \frac{r(h-1)}{2}\right)}{P_\lambda hN(N-1)}\right) \quad (47)$$

Generally, when the bidirectional traffic demand volume is randomly distributed, the case of equal average traffic demands has better power efficiency compared to the random demand case. For random traffic demands, Equation 43 is rewritten as:

$$\tilde{P} = \sum_{s\in N}\sum_{\substack{d\in N \\ d<s}} 2\max(P_\lambda^{sd}, P_\lambda^{ds}) + \max(P_\lambda^{sd}, P_\lambda^{ds}) r(h^{sd} - 1) \quad (48)$$

Where the first term is responsible for the power consumption at end nodes which uses conventional ports, and the second term is responsible for the power consumption at intermediate nodes which make use of NC ports. Demands are treated in pairs; this is the reason $(d < s)$ is introduced under the summation and also the equation being multiplied by two. Hence, $max(P_\lambda^{sd}, P_\lambda^{ds})$ can be rewritten as:

$$max\left(P_\lambda^{sd}, P_\lambda^{ds}\right) = \left(\frac{P_t + P_x}{B}\right)(\lambda^{sd}, \lambda^{ds}) \quad (49)$$

$$max(\lambda^{sd}, \lambda^{ds}) = \max(\lambda + \Delta^{sd}, \lambda + \Delta^{ds}) = \lambda + \max(\Delta^{sd}, \Delta^{ds}) \quad (50)$$

Where λ denotes the average traffic of the entire network. Thus, the total power of the NC scenario can be expressed as:

$$\tilde{P} = 2\left(\frac{P_p + P_t}{B}\right)\sum_{s\in N}\sum_{\substack{d\in N \\ d<s}}[\lambda + max(\lambda^{sd}, \lambda^{ds})]\left[1 + r\frac{h^{sd}-1}{2}\right] \quad (51)$$

Which can be expressed as:

$$\tilde{P} = P_\lambda N(N-1)\left[1 + r\frac{h-1}{2}\right] + 2\left(\frac{P_p + P_t}{B}\right)\sum_{s\in N}\sum_{\substack{d\in N \\ d<s}} max(\Delta^{sd}, \Delta^{ds})\left[1 + r\frac{h^{sd}-1}{2}\right] \quad (52)$$

Where the first and second components of Equation 3.50 represent the power consumption of the network coded case, when the traffic demand all equate to average. Let $\widetilde{P^1}$ and $\widetilde{P^2}$ denote the first part and the second part of Equation 52, respectively. Then,

$$\widetilde{P^1} = P_\lambda N(N-1)\left[1 + r\frac{h-1}{2}\right] \quad (53)$$

$$\widetilde{P^2} = 2\left(\frac{P_p + P_t}{B}\right)\sum_{s\in N}\sum_{\substack{d\in N \\ d<s}} max(\Delta^{sd}, \Delta^{ds})\left[1 + r\frac{h^{sd}-1}{2}\right] \quad (54)$$

If H_k denotes a set of demands with minimum hop paths of k hops, then Equation 54 can be re-written as:

$$\widetilde{P^2} = \frac{P_p + P_t}{B}\left[r\sum_{\substack{(s,d)\in H_2 \\ d<s}} max(\Delta^{sd}, \Delta^{ds}) + 2r\sum_{\substack{(s,d)\in H_3 \\ d<s}} max(\Delta^{sd}, \Delta^{ds}) + \cdots + (k-1)r\sum_{\substack{(s,d)\in H_k \\ d<s}} max(\Delta^{sd}, \Delta^{ds})\right] + 2\frac{P_p + P_t}{B}\sum_{s\in N}\sum_{\substack{d\in N \\ d<s}} max(\Delta^{sd}, \Delta^{ds}) \quad (55)$$

Given that $g_z(\lambda^{sd}) = max(\Delta^{sd}, \Delta^{ds})$, then,

$$\widetilde{P^2} = \left(\frac{P_p + P_t}{B}\right)\left[\sum_k \sum_{(s,d)\in H_k} (k-1) r g_z(\lambda^{sd}) + 2\sum_{s\in N}\sum_{\substack{d\in N \\ d<s}} g_z(\lambda^{sd})\right] \quad (56)$$

The given topology (reflected in H_k) and the given traffic volume distribution $g_z(\lambda^{sd})$ determines the value of $\widetilde{P^2}$. This results in three lower bounds. First by setting all hop counts to minimum, second, by setting the traffic to a value that reduces the total power, and finally, setting the hop count and the traffic component to their minimum values. The similar effect applies to the three upper bounds.

The bounds for total power are defined as: For any given topology, the minimum value is defined when $g_z(\lambda^{sd}) = max(\Delta^{sd}, \Delta^{ds}) = 0$ when $\Delta^{sd} = \Delta^{ds} = 0$. It should be noted that these values are reached when demands are equal. This results in the expression of $\tilde{P}$ as:

$$\tilde{P} \geq P_\lambda N(N-1)\left(1 + r\frac{h-1}{2}\right) \quad (57)$$

The effect of Equation 57 reduces the scenario to the previous scenario of equal average demands.

In order to attend a generic traffic demand and optimal topology, the following minimum value is reached when all demands have a single hop route ($h = 1$) when the network is connected in full mesh.

$$\tilde{P} \geq P_\lambda N(N-1) \quad (58)$$

This implies that power consumption is directly proportional to the variation. It is worthy to state also that, when a set of traffic demand is given with variation, the lowest power consumption is attained when bidirectional demands with the highest variance is allocated to the route with minimum hop count. Similarly, the maximum value of $\widetilde{P^2}$ can be computed by considering the topology and traffic dimensions. Consider the traffic dimension beginning from Equation 48 with the fact that $\max(P_\lambda^{sd}, P_\lambda^{ds}) \leq \frac{P_p + P_t}{B}\lambda_{max}$ where λ_{max} denotes the upper limit of the traffic value, supposing there is uniform traffic distribution

$$\tilde{P} \leq 2\frac{P_p + P_t}{B}\lambda_{max}\sum_{s\in N}\sum_{\substack{d\in N \\ d<s}}\left[1 + r\frac{h^{sd}-1}{2}\right] \quad (59)$$

This results in:

$$\tilde{P} \leq \frac{P_p + P_t}{B}\lambda_{max} N(N-1)\left[1 + r\frac{h-1}{2}\right] \quad (60)$$

Upper bound regarding maximum hop count and the exact is achieved by setting the hop count for each demand to the highest in the network. This implies that $h^{s,d} = h_{max}$ in Equation 54 will result in:

$$\widetilde{P^2} \leq 2\left(\frac{P_p + P_t}{B}\right)\left[1 + r\frac{h_{max}-1}{2}\right]\sum_{s\in N}\sum_{\substack{d\in N \\ d<s}} g_z(\lambda^{sd}) \quad (61)$$

Hence, the bound for the total power consumption is transformed to:

$$\tilde{P} \leq P_\lambda N(N-1)\left(1 + r\frac{h-1}{2}\right) + 2\left(\frac{P_p + P_t}{B}\right)\left[1 + r\frac{h_{max}-1}{2}\right]\sum_{s\in N}\sum_{\substack{d\in N \\ d<s}} g_z(\lambda^{sd}) \quad (62)$$

If both the maximum traffic and hop count are considered, the following bound is certain.

$$\tilde{P} \leq \frac{P_p + P_t}{B}\lambda_{max} N(N-1)\left[1 + r\frac{h_{max}-1}{2}\right] \quad (63)$$

The upper bound derived by considering the maximum hop count is more compact than the one considering the maximum possible traffic demand, due to the lower variance the top count has with respect to the traffic demand variance.

For the partitioning approach, a closed from expression is developed the same way as the zero padding approach. The number of NC ports X in the network for partitioning scenario is expressed as:

$$X = \frac{1}{B}\sum_{s\in N}\sum_{\substack{d\in N \\ d<s}} \min(\lambda^{sd}, \lambda^{ds})(h^{sd} - 1) \quad (64)$$

The traffic at source and destination nodes and the remaining traffic at the partitioning process at intermediate nodes will be covered by the number of conventional ports. Thus,

$$Y = \frac{1}{B}\left(\sum_{s\in N}\sum_{\substack{d\in N \\ d<s}} \lambda^{sd} + \sum_{s\in N}\sum_{\substack{d\in N \\ d<s}} (h^{sd} - 1)(|\lambda^{sd} - \lambda^{ds}|)\right) \quad (65)$$

and the total power is expressed as:

$$P_t = \frac{P_x + P_t}{B}\sum_{s\in N}\sum_{\substack{d\in N \\ d<s}} \min(\lambda^{sd}, \lambda^{ds})(h^{sd} - 1) + \frac{P_p + P_t}{B}\sum_{s\in N}\sum_{\substack{d\in N \\ d\neq s}} \lambda^{sd} + \frac{P_p + P_t}{B}\sum_{s\in N}\sum_{\substack{d\in N \\ s<d}} (h^{sd} - 1)(|\lambda^{sd} - \lambda^{ds}|) \quad (66)$$

Combining the terms results in:

$$P_t = \frac{P_p + P_t}{B}\sum_{s\in N}\sum_{\substack{d\in N \\ d\neq s}} \lambda^{sd} + \sum_{s\in N}\sum_{\substack{d\in N \\ d<s}} (h^{sd} - 1)\left(\frac{P_x + P_t}{B} min(\lambda^{sd}, \lambda^{ds}) + \frac{P_p + P_t}{B}(|\lambda^{sd} - \lambda^{ds}|)\right) \quad (67)$$

The terms in Equation 67 can be rearranged to have:

$$P_t = \frac{P_p + P_t}{B} N(N-1)\lambda + \frac{P_p + P_t}{B}\sum_{s\in N}\sum_{\substack{d\in N \\ d<s}} (h^{sd} - 1)\left(r \times min(\lambda^{sd}, \lambda^{ds}) + (|\lambda^{sd} - \lambda^{ds}|)\right) \quad (68)$$

$$P_t = \frac{P_p + P_t}{B} N(N-1)\lambda + \frac{P_p + P_t}{B}\sum_{s\in N}\sum_{\substack{d\in N \\ d<s}} (h^{sd} - 1)\left[\Delta + r \times min(\lambda^{sd}, \lambda^{ds})\right] \quad (69)$$

Note that $\Delta = |\lambda^{sd} - \lambda^{ds}| = max(\lambda^{sd}, \lambda^{ds}) - min(\lambda^{sd}, \lambda^{ds})$. Substituting this is Equation 69 results in:

$$P_t = \frac{P_p + P_t}{B} N(N-1)\lambda + \frac{P_p + P_t}{B}\sum_{s\in N}\sum_{\substack{d\in N \\ d<s}} (h^{sd} - 1)\left[max(\lambda^{sd}, \lambda^{ds}) - min(\lambda^{sd}, \lambda^{ds}) + r \times min(\lambda^{sd}, \lambda^{ds})\right] \quad (70)$$

Collecting like terms results in:

$$P_t = \frac{P_p + P_t}{B} N(N-1)\lambda + \frac{P_p + P_t}{B}\sum_{s\in N}\sum_{\substack{d\in N \\ d<s}} (h^{sd} - 1)\left[max(\lambda^{sd}, \lambda^{ds}) + (r-1)min(\lambda^{sd}, \lambda^{ds})\right] \quad (71)$$

Let $g_p(\lambda^{sd})$ denotes the maximum traffic imbalance in a network where the network coding ports and conventional ports consume same amount of power. $g_p(\lambda^{sd})$ is defined as:

$$g_p(\lambda^{sd}) = max(\lambda^{sd}, \lambda^{ds}) + (r-1)min(\lambda^{sd}, \lambda^{ds}) \quad (72)$$

The total power can further be modified as:

$$P_t = \frac{P_p + P_t}{B} N(N-1)\lambda + \frac{P_p + P_t}{B}\sum_{s\in N}\sum_{\substack{d\in N \\ s<d}} (h^{sd} - 1)\, g_p(\lambda^{sd}) \quad (73)$$

If the Equation 72 is minimized, the lower bound considering the traffic dimension can be obtained.

$$g_{pmin}(\lambda^{sd}) = \bar{\lambda}^{sd} + (r-1)\bar{\lambda}^{sd} = r\bar{\lambda}^{sd} \quad (74)$$

$\bar{\lambda}^{sd}$ is the traffic volume between (s, d) when the maximum value is the same as the minimum value and the average. The total power can now be expressed as:

$$P_t = \frac{P_p + P_t}{B} N(N-1)\lambda + \frac{P_p + P_t}{B}\sum_{s\in N}\sum_{\substack{d\in N \\ s<d}} (h^{sd} - 1)\,\bar{\lambda}^{sd} r \quad (75)$$

By introducing the Chebyshev's inequality presented in Equation 76, where a lower bound on the average of the inner product of two vectors of size n is given as:

$$\frac{1}{n}\sum_{k=1}^{n} a_k b_k \geq \left(\frac{1}{n}\sum_{k=1}^{n} a_k\right)\left(\frac{1}{n}\sum_{k=1}^{n} b_k\right) \quad (76)$$

Equation 75 becomes:

$$P_t \geq \frac{P_p+P_t}{B}N(N-1)\lambda + \frac{P_p+P_t}{B}\sum_{k=1}^{\frac{N(N-1)}{2}} \frac{1}{\frac{N(N-1)}{2}}(h^k - 1)\sum_{k=1}^{\frac{N(N-1)}{2}} r\bar{\lambda}^k \quad (77)$$

Further reducing the second term of the inequality in Equation 77 yields:

$$P_t \geq \frac{P_p+P_t}{B}N(N-1)\lambda + \frac{P_p+P_t}{B}\left[\frac{1}{\frac{N(N-1)}{2}}\left(h\frac{N(N-1)}{2} - \frac{N(N-1)}{2}\right)r\lambda\frac{N(N-1)}{2}\right] \quad (78)$$

Equation 78 is further reduced to:

$$P_t \geq \frac{P_p+P_t}{B}N(N-1)\lambda\left[1+(h-1)\frac{r}{2}\right] \quad (79)$$

The topology dimension is now considered:

$$P_t \geq P_\lambda N(N-1) + \frac{P_p+P_t}{B}(h_{min}-1)\sum_{s\in N}\sum_{\substack{d\in N\\ s<d}} g_p(\lambda^{sd}) \quad (80)$$

Note that $h_{min} = 1$

$$P_t \geq P_\lambda N(N-1) \quad (81)$$

Considering the topology dimension, the upper bound is given by:

$$P_t \leq P_\lambda N(N-1) + \frac{P_p+P_t}{2B}(h_{max}-1)\sum_{s\in N}\sum_{\substack{d\in N\\ s<d}} g_p(\lambda^{sd}) \quad (82)$$

Consider the traffic dimension and also bear in mind the fact that the maximum power consumption of the network under network coding takes place when network coding is not in use. For the partitioning approach, when the bidirectional traffic is fully asymmetric, this implies that, in one direction, $\lambda^{sd} = \lambda_{max}$, and in the other direction, $\lambda^{sd} = 0$; network coding is not used in this case. Then Equation 73 transforms to:

$$P_t \leq P_\lambda N(N-1) + \frac{P_p+P_t}{B}\lambda_{max}\sum_{s\in N}\sum_{\substack{d\in N\\ s<d}}(h^{sd}-1) \quad (83)$$

Which results in:

$$P_t \leq N(N-1)\frac{P_p+P_t}{B}\left[\lambda + \lambda_{max}\frac{h-1}{2}\right] \quad (84)$$

When the maximum traffic in the network and the largest hop count are considered, the upper bound expressed in Equation 86 is obtained. The upper bounds definition is essential the topology and traffic can have varying performance. Generally, the bound with maximum traffic volume is higher than the one with maximum hop count. However, in the case of network with very large hop count and flat traffic, the opposite is happens.

$$P_t \leq P_\lambda N(N-1) + \frac{P_p+P_t}{B}(h_{max}-1).\lambda_{max}\frac{N(N-1)}{2} \quad (85)$$

$$P_t \leq P_\lambda N(N-1) + \frac{P_p+P_t}{B}\left[\lambda + \lambda_{max}\frac{h_{max}-1}{2}\right] \quad (86)$$

It should be noted that the power consumption obtained by network coding with traffic partitioning approach and equal traffic demands between all node pairs as given in Equation 80 is equal to the one given by zero padding approach also considering equal traffic demands. Similarly, the lower bounds are the same in both cases, when optimizing topology, giving full mesh which yields no contribution from the network coding, and the minimal traffic case when both bidirectional flows are equal to the average.

3. Results and Discussion

3.1 Network Performance Evaluation

Regular and common topologies were used in the analysis of energy efficient **IP over Wavelength-Division Multiplexing (WDM) network model presented in** this work. For regular topologies, the ring, line, star and full mesh options were analyzed. For real world core network, the SkyRock network system (which in this work is subsequently referred to as "SKYNET") and the ENIAC Data services network system (which in this work is subsequently be referred to as "ENIACNET) were considered. These two referenced companies are located in Uyo, Akwa Ibom State, Nigeria. The SKYNET, as shown in Figure 7 has 14 nodes and 21 links and an average hop count of 2.17, while the ENIACNET, as shown in Figure 8 has 24 nodes and 43 links with an average hop count of 3.

The traffic demand was evaluated using the average network traffic demand at various times of the day, according to a uniform distribution with values ranging from 20Gb/s to 120Gb/s.

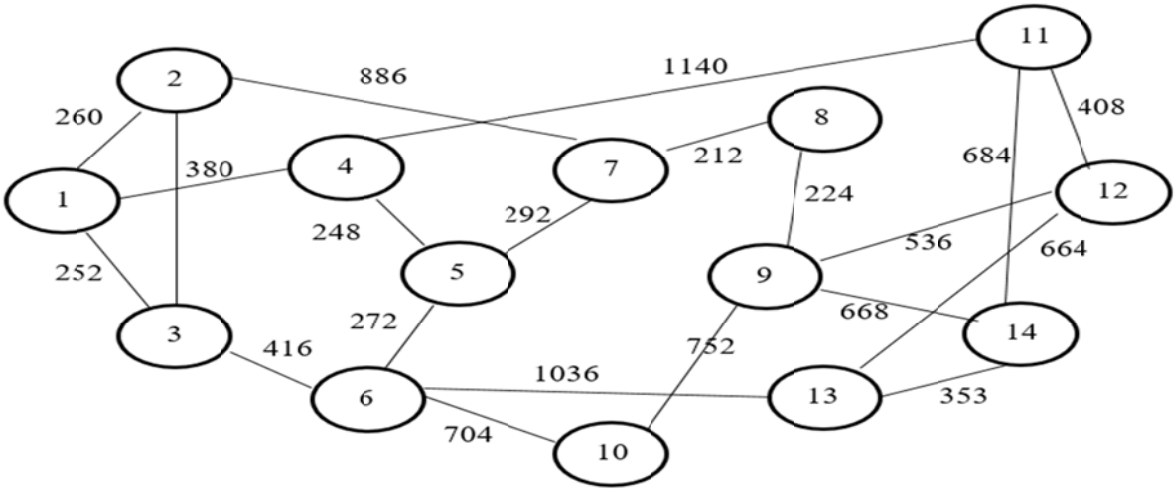

Figure 7: The SKYNET topology

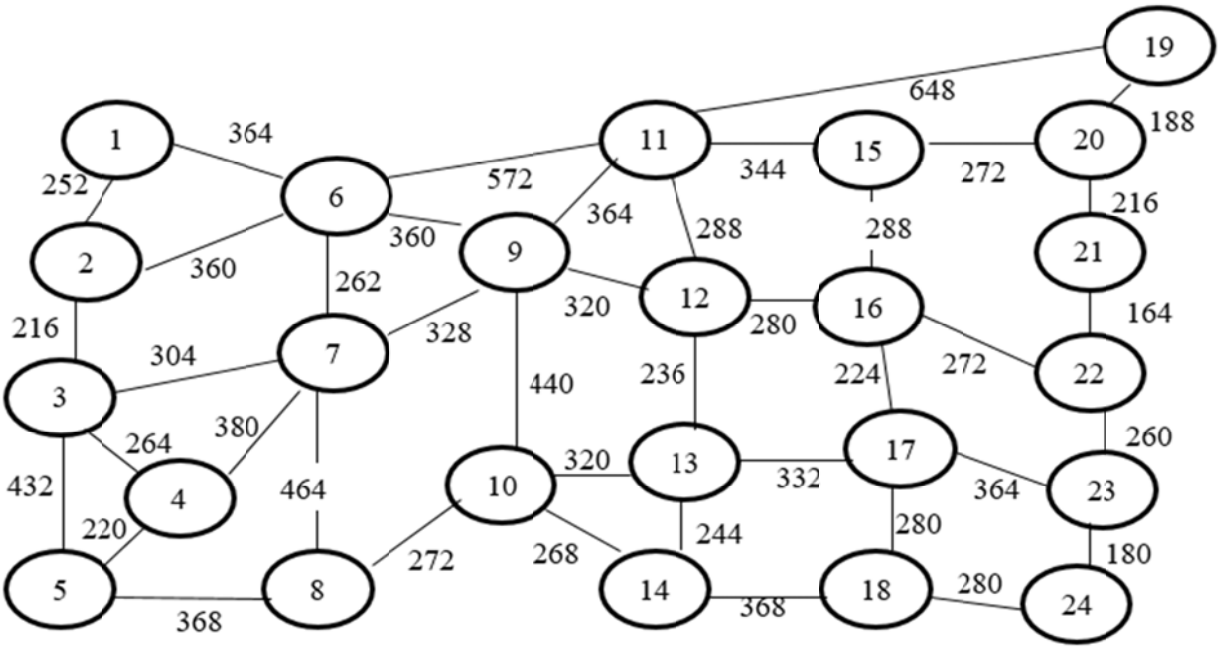

Figure 8: The ENIACNET topology

The actual traffic is arbitrarily generated with the average traffic as shown in Figure 9. The traffic model portrays two types of variations; the first one is between different times of the day, while the second one is between different nodes at a given time point. The traffic demand between node pair assumes values between 10 and 230 Gbps. Other network parameters including power consumption of different components are shown in Table 1. The power consumption of the network components are taken from [2], [3], [5], [9], [10]. The increase in power consumption for NC ports implies that there is a good estimate of power consumption of the processing of XOR operation and the additional amplifier and transmitter at the physical interface module port. This estimate agrees with the architecture of Cisco Carrier Routing System [2], where the router consists of multiple line cards connected through switch fabrics, and each line card is composed of an interface module that performs layer 1 and layer 2 functionality of the network, and a modular service card that performs layer 3 processing and forwarding. This increased network power consumption considers the fact that the majority of the router port will not change such as the switching fabric, packet's header processing and look up table reading. During computation, a partially used wavelength was assumed to consume part of a router port and a transponder proportional to traffic volume. The assumption here is that either grooming or a proportional power profile for router ports and transponders and such a proportional power profile is advantageous and is a goal of current equipment manufacturers and it is realistic to achieve grooming.

The MILP optimization was performed using the ANYLOGIC software running on a high performance computing cluster with 16 cores CPU and 256GB RAM. The energy efficient routing heuristic deployed in this research can be described by routing all demands based on the minimum hop path between the source and destination, selecting the shortest path in case two alternative path have the same minimum hop. Judging from this flow allocation, network coding is carried out at all intermediate nodes, the total power consumption and the quantity of conventional ports and NC ports are computed.

Table 1: Network parameters

Parameter	Value
Distance between neighboring erbium-doped fiber amplifiers (EDFAs)	8m
Number of wavelength in fiber (W)	16
Capacity of each wavelength (B)	40Gbps
Power consumption of a normal port (Pp) [2]	1kW
Power consumption of a coded port (Px)	1.1kW
Power consumption of a transponder (Pt) [3]	73W
Power consumption of an optical switch PO [5]	85W
Power consumption of a MUX/DeMUX [9]	102W
Power consumption of EDFAs (Pe) [10]	8W

Figure 9 and Figure 10 depicts the power consumption of SKYNET and ENIACNET topologies, at different times of the day, respectively. It is shown that by introducing network coding to SKYNET and ENIACNET topologies, daily average power savings of 27% and 33% are obtained respectively. It should be noted that there is a limited effect in terms of increase in power savings on the ENIACNET topology due to the higher average hop count. Although a higher hop count implies that NC ports will replace more conventional ports, however, it also implies that more conventional ports are needed to establish flows between nearby nodes where traffic flows cannot be encoded. The ratio of the traffic between neighboring nodes (which cannot be encoded) and the non-neighboring nodes (which

can be encoded) determines the total power savings obtained by network coding.

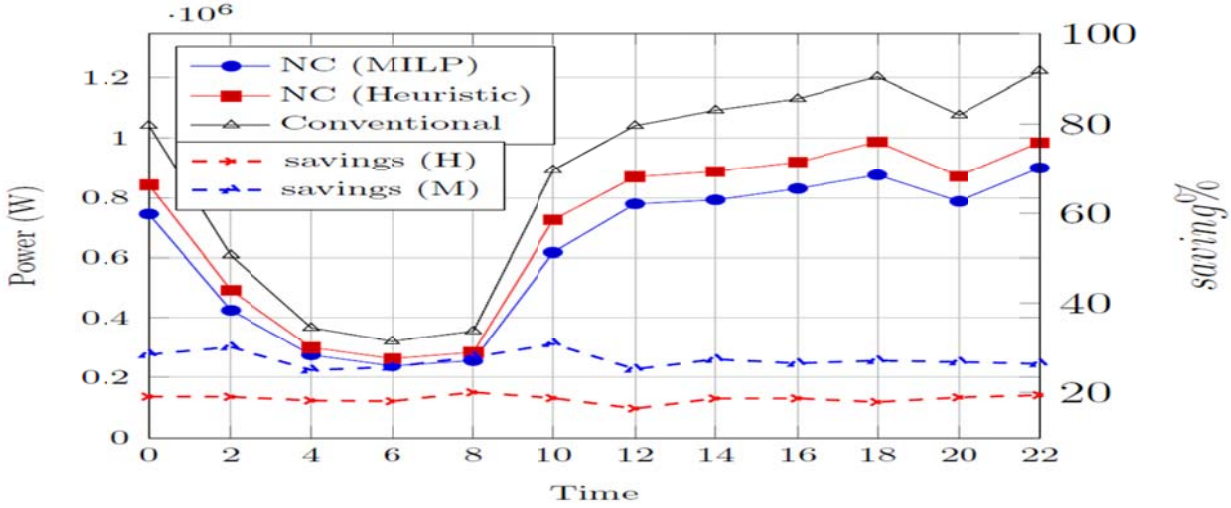

Figure 9: Power consumption of the SKYNET network with and without network coding

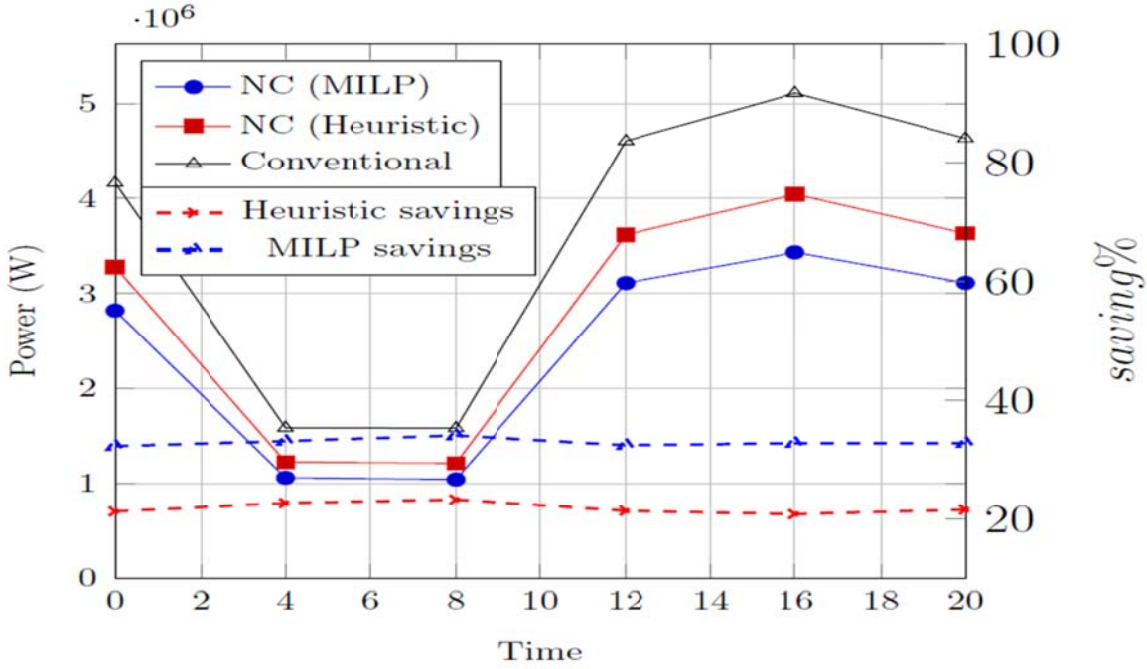

Figure 10: Power consumption of the ENIACNET network with and without network coding

More savings can be achieved for networks of high hop counts as discussed below.

The comparison of distribution of conventional ports and NC ports across SKYNET nodes is shown in Figure 11. The NC ports are used more in the middle of the network at nodes with high nodal degree while the conventional ports are almost equally distributed among the network nodes. This is attributed to the fact that middle nodes are more likely to serve as intermediate traffic nodes. It is also seen that node 6 has the highest number of NC ports since it is located at the center of the network with a nodal degree of 4. It should be noted that nodes with lower hop count and/or not located at the center deploy smaller number of NC ports.

There is no deviation from the minimum hop routes selected by the conventional scenario for the routes selected by the solution of the MILP model. This fact can make it possible to migrate to new architecture. Hence, the quantity of the required coded port at each node can be estimated at design time. From Figure 9 and Figure 10, it is shown that average power savings obtained by the energy efficient routing heuristic in network where coding is enabled (19% and 22% considering SKYNET and ENIACNET networks, respectively) tends to level up with those of the energy efficient network coding.

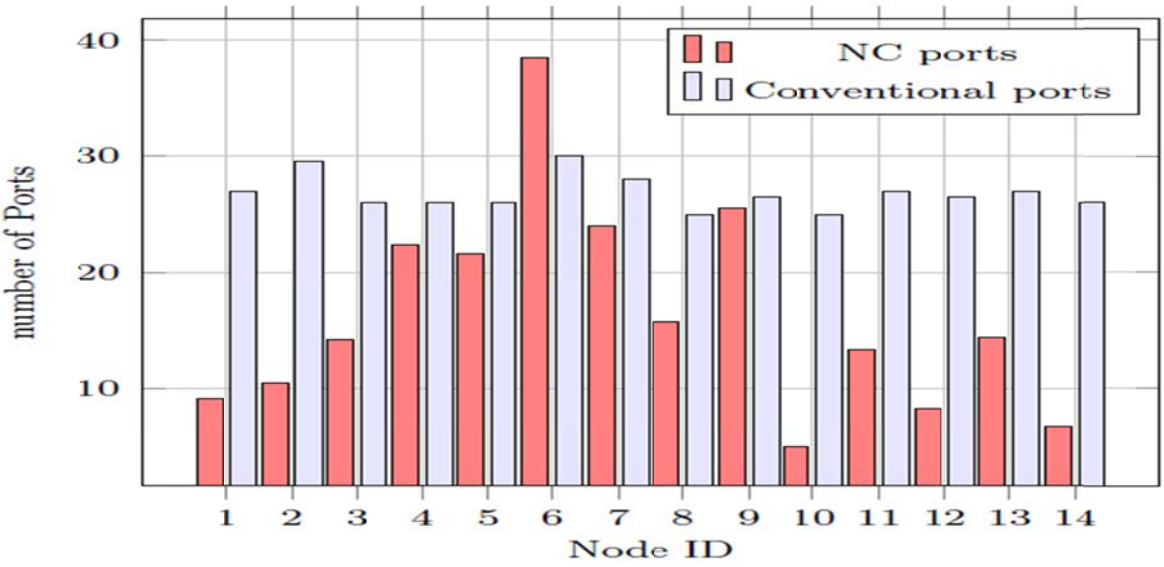

Figure 11: Comparison between the number of the two types of ports in SKYNET nodes

The performance of the energy efficient network coding scenario under a traffic profile based on the gravity model where the traffic production volume and appealing nature of each node is proportional to the population of that node is also analyzed. The traffic demands between node pairs were normalized to obtain averages. The results in Figure 11 depict that daily average savings is obtained up to 22% when applied on the SKYNET.

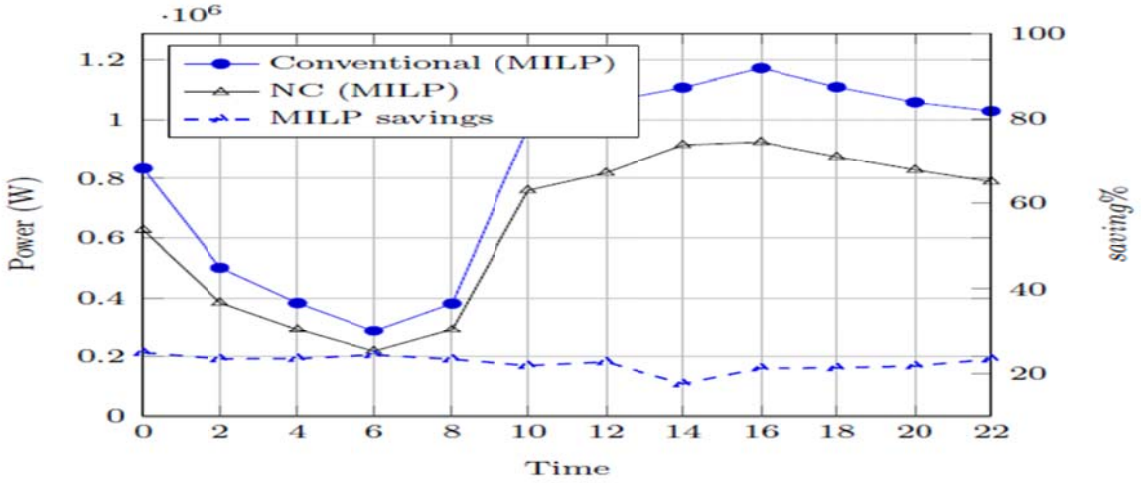

Figure 12: Power consumption of SKYNET network with and without network coding using gravity model

network model as depicted in Figure 13 and Figure 14 respectively.

3.2 Regular Topologies Impact on Model

In order to evaluate the impact of topology, the SKYNET network is reconfigured into a bidirectional ring, and a star

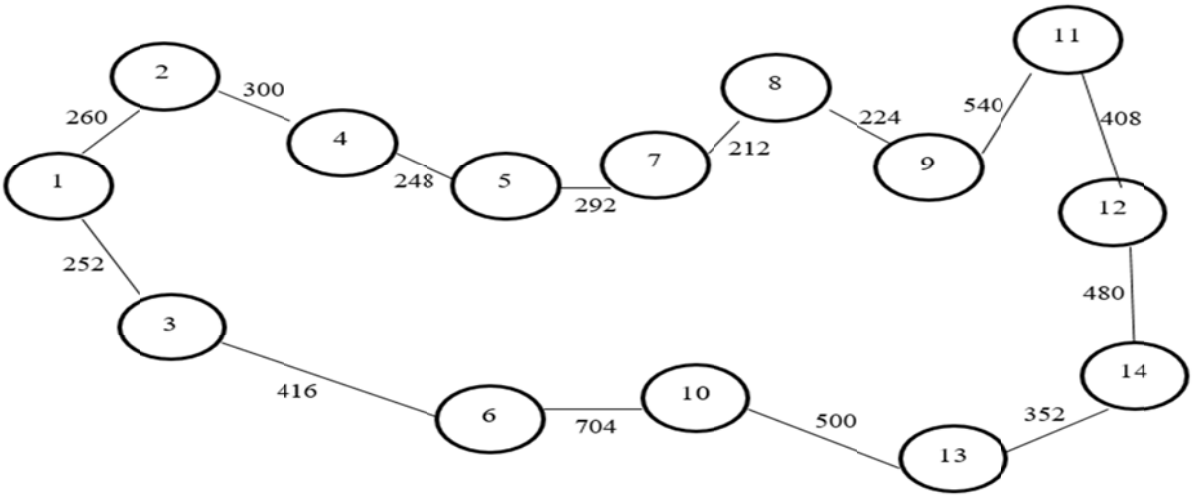

Figure 13: The SKYNET connected by ring topology

If line 12-14 is removed in Figure 13, a line topology is formed. It should be noted that a star topology can be realistic if the network is dominated by traffic due to large data centers. If the key metrics are considered to be power consumption and delay, then full mesh can be an attractive network topology. The line and ring topologies were considered since they have high average loop count. The distances displayed on the links were arbitrarily estimated based on nodes locations. The highest reduction in network power consumption (about 33% daily savings) in the line topology is contributed by network coding. It can also be inferred that the high power saving of the line topology is due to its high average hop count of 5, increasing the number of intermediate nodes, which in turn increases the number of conventional ports to be replaced by the NC ports.

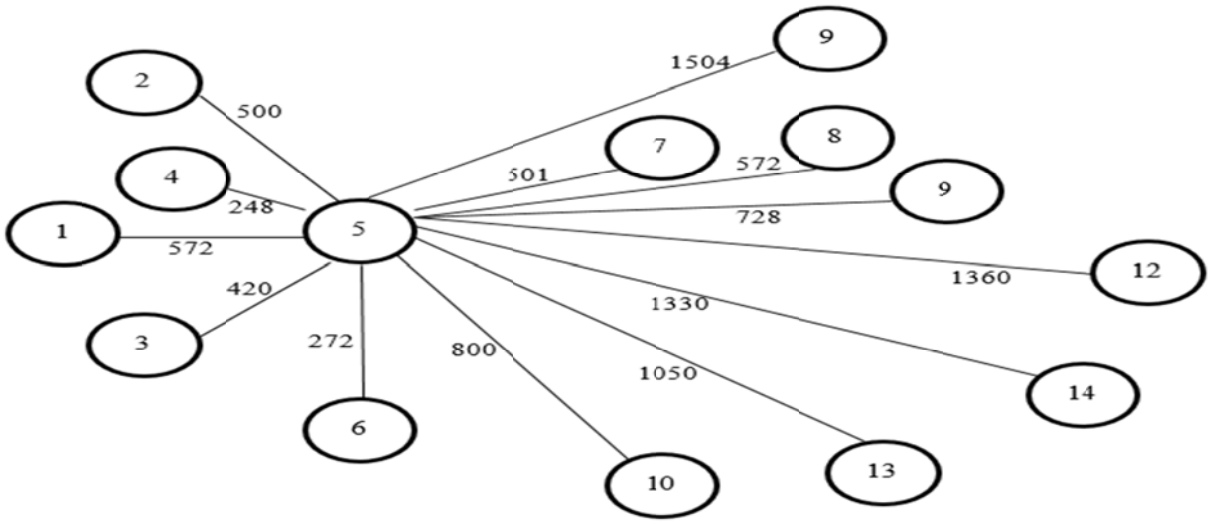

Figure 14: The SKYNET connected by star topology

On the other hand, network coding attributes no peculiar advantage to the full mesh topology, since all the demands are routed through single hop routes. The savings achieved by the two other topologies lives between these two extremes. Introducing network coding into a bidirectional ring topology (with average hop count of 3.77) has saved 30% of the network power consumption whereas the star topology centered at node 5 with an average hop count of 1.85 has saved 16% of the network power consumption.

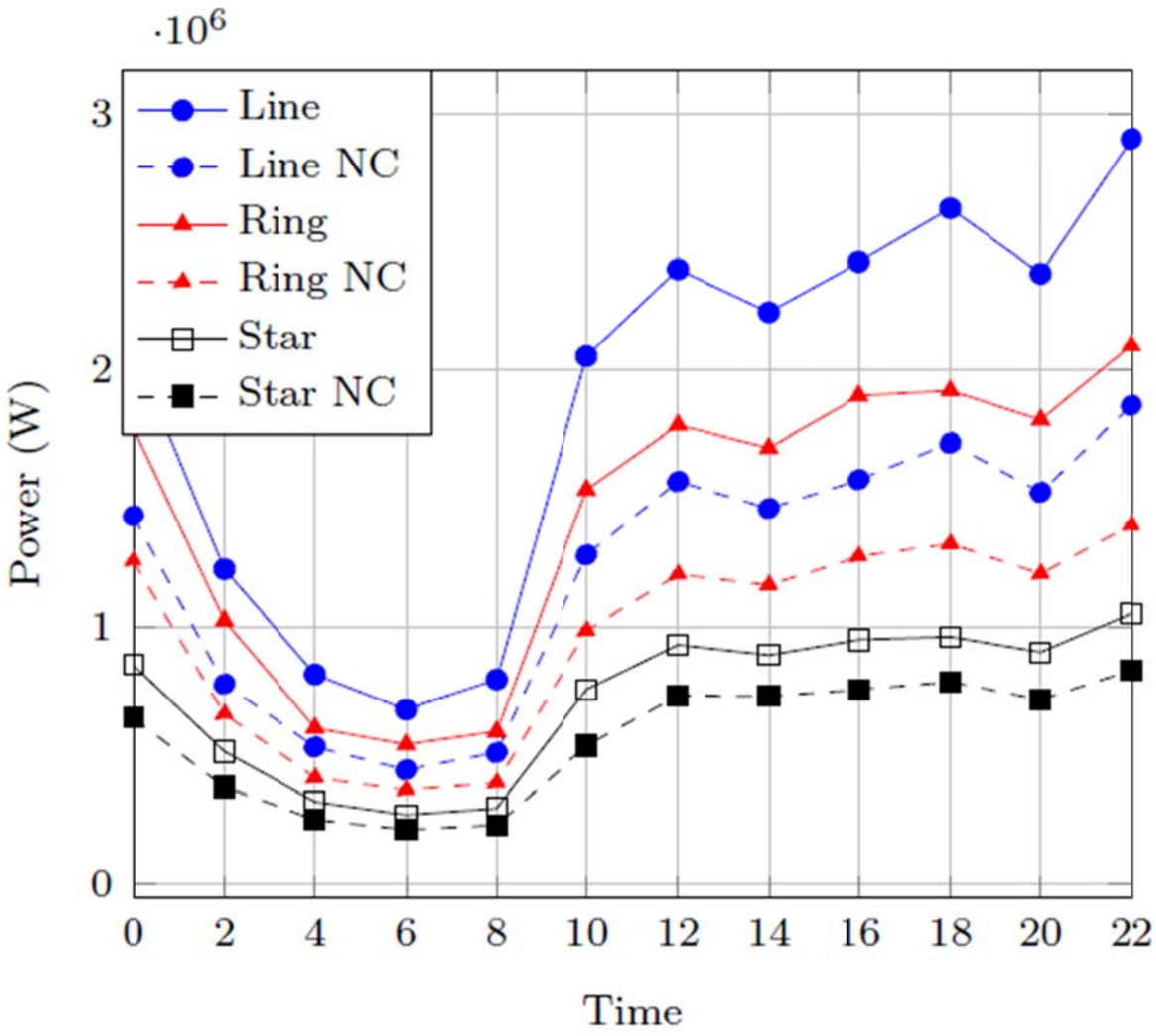

Figure 15: Power consumption of the ring and star topologies with and without network coding (MILP results)

The considered topologies in this research vary from full mesh topology having the maximum number of links to the star topology having the minimum number of links which maintaining connectivity.

All the results presented above are based on the estimation of NC port power consumption given in Equation 1 to Equation 8. Figure 17 depicts how the savings achieved by network coding are affected as r (the ratio of the network coding scheme power consumption (i.e. transponders and router ports) and conventional scheme) grows. The achieved savings reduces compared to conventional scenario as r increases.

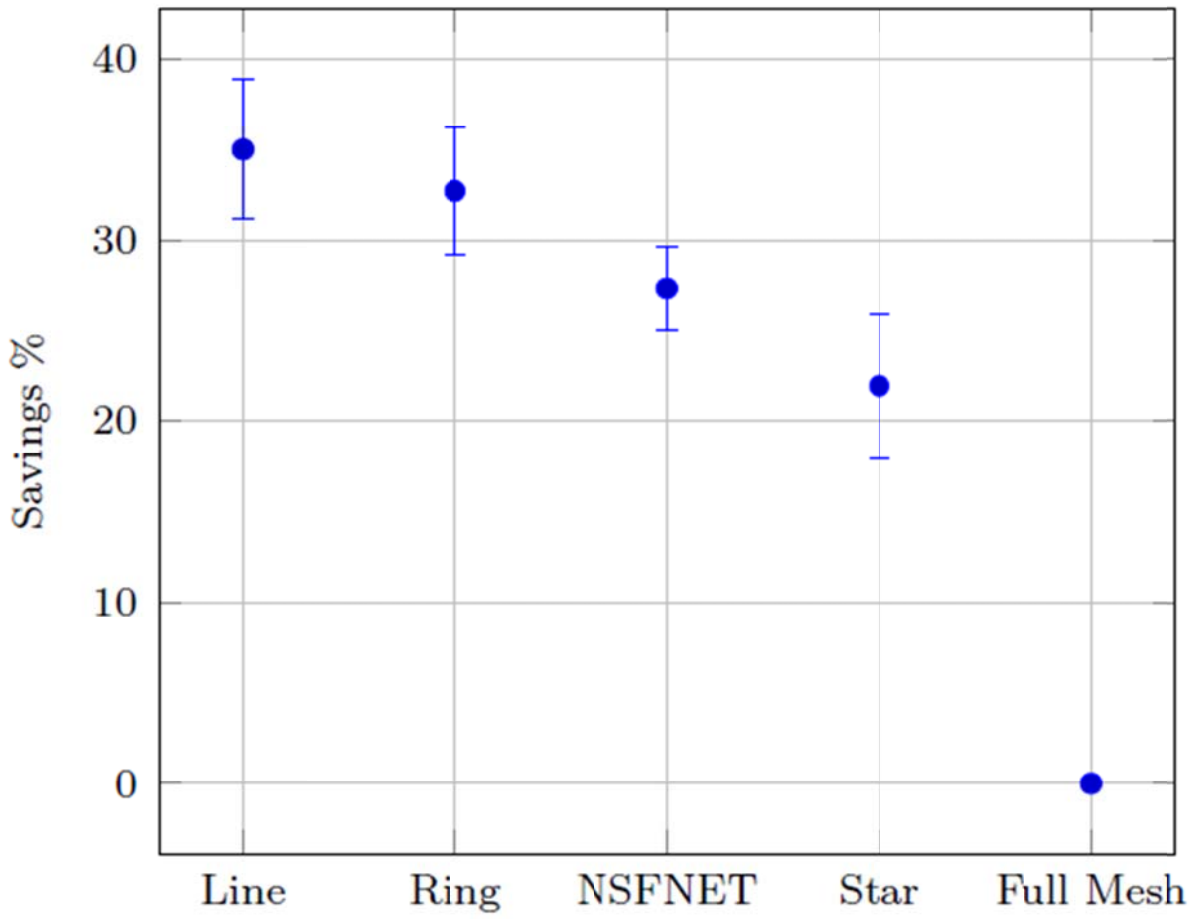

Figure 16: Maximum, minimum, and average daily power savings in different network coded topologies.

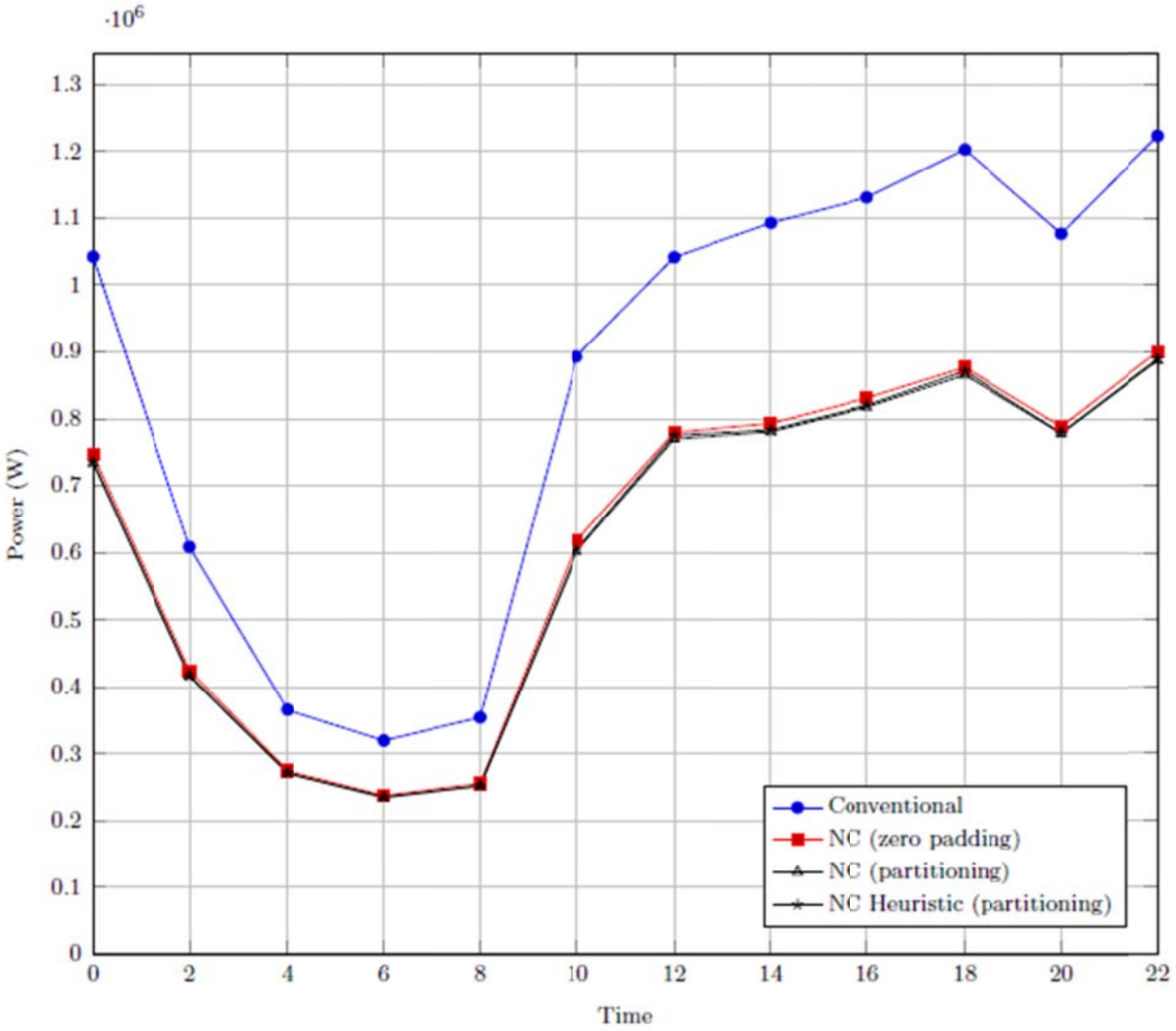

Figure 17: Power consumption of SKYNET under network coding with partitioning approach

The dependence of power consumption in network coding case on the ports ratio $r = \frac{P_t + P_x}{P_p + P_t}$ for network coding and conventional case with packet partitioning and zero padding under random traffic using MILP model is depicted in Figure 18. It shows that savings is impacted by port ratio, which are better in a scenario of packet partitioning (shown in Figure 6). Savings is observed as long as NC port (including transponders) power consumption is less than twice that of the conventional port power consumption.

In Figure 19, power consumption of network is plotted for different network coding transponder power consumption values while the conventional transponder power consumption remain constant to make up for the uncertainty in the additional power consumption that is required to implement the additional functions related to network coding. This type of sensitivity analysis helps in determining the maximum allowable power consumption for network coded transponder, where the network coding still produces power saving compared to other approaches.

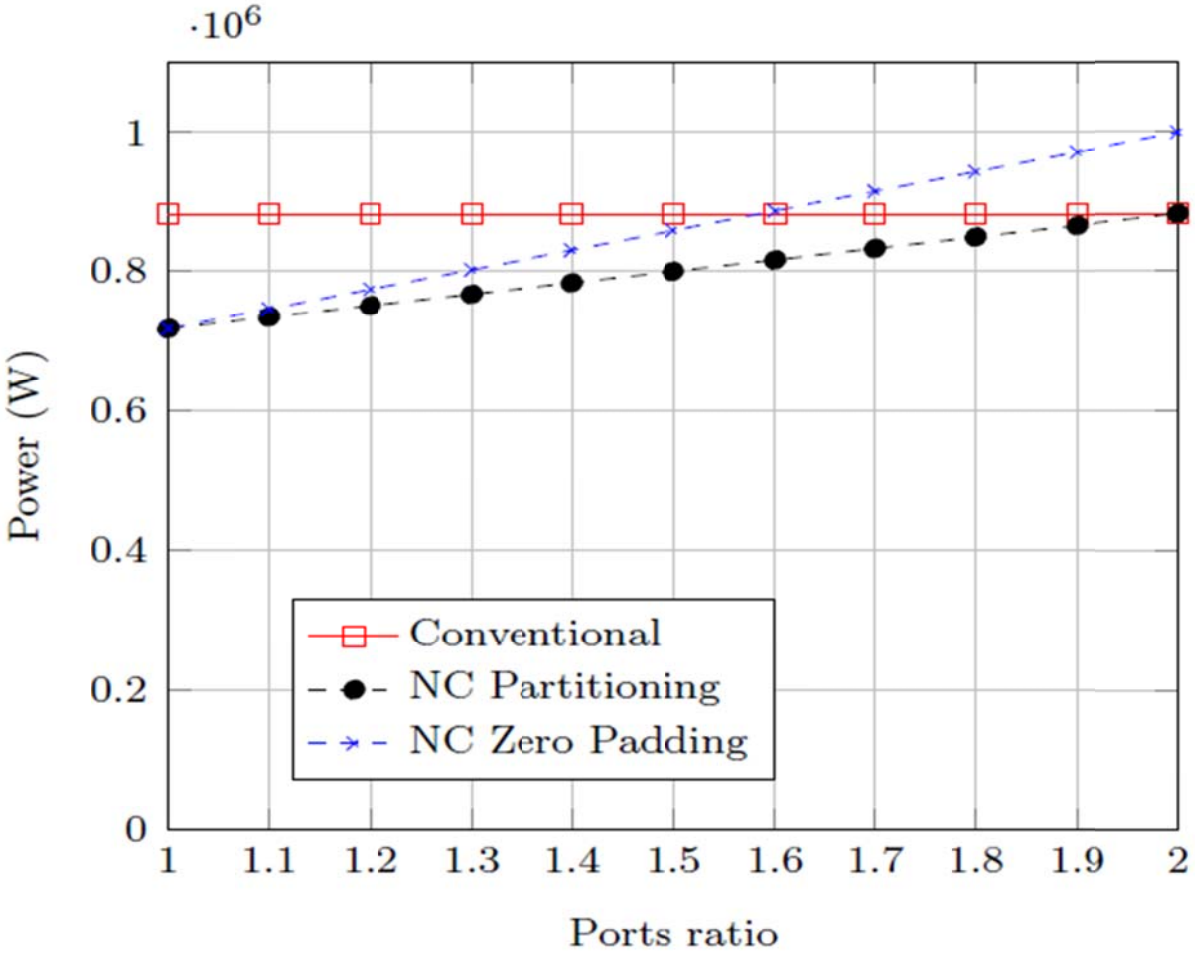

Figure 18: Power consumption against port ratio using MILP model

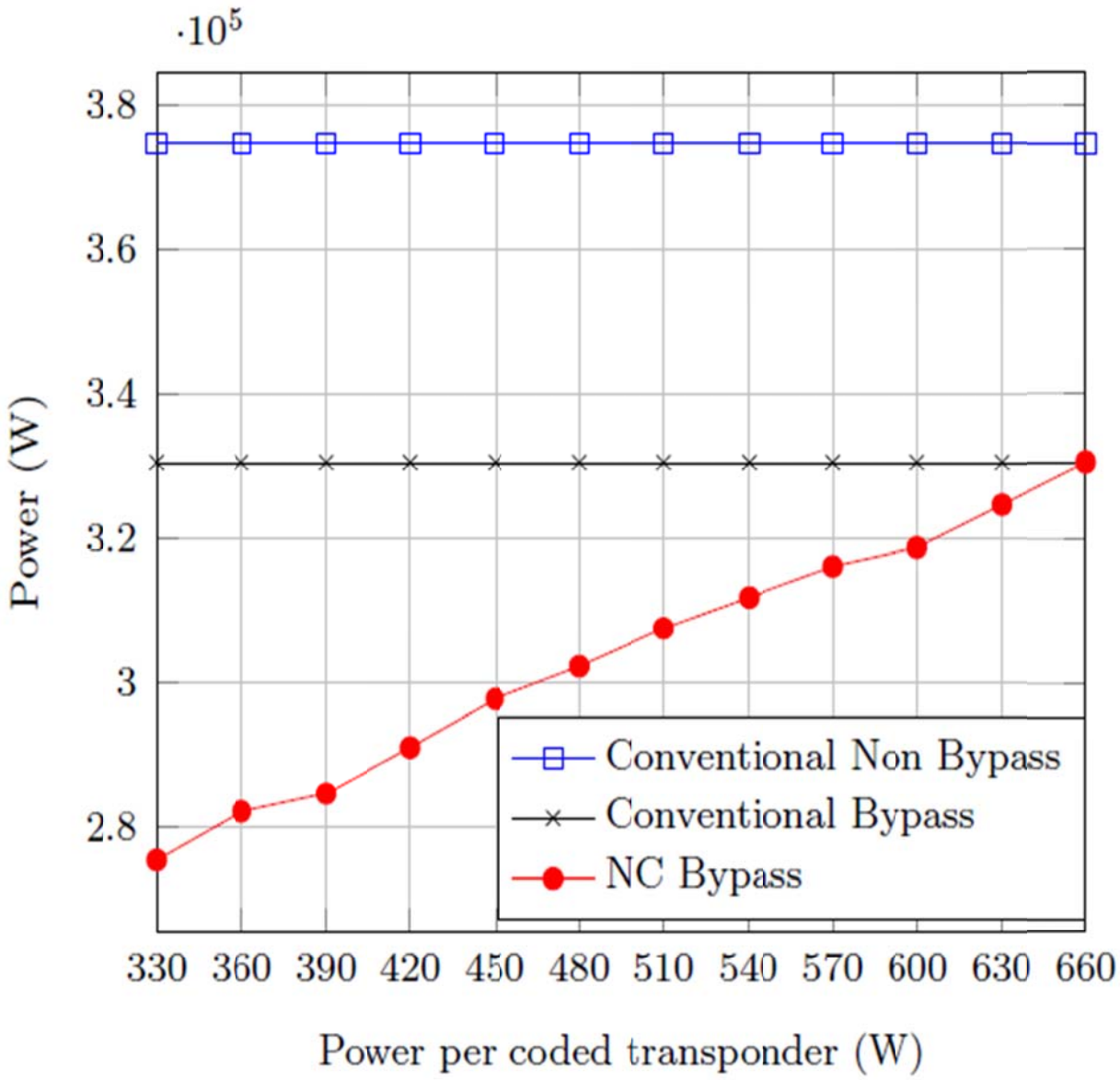

Figure 19: Power consumption of network for different coded transponders' power values

Recall in Equation 47 , that power savings was given as $\phi = 1 - \frac{\bar{P}}{P} = 1 - \left(\frac{P_\lambda N(N-1)\left(1+\frac{r(h-1)}{2}\right)}{P_\lambda hN(N-1)}\right)$ which was further reduced to

$$\phi = \left(1 - \frac{1 + 0.5r(h-1)}{h}\right)$$

Using the power consumption parameters of the conventional ports and NC ports provided in Table 1, and given $r \approx 1.1$, then the savings expression is reduced to:

$$\phi = \left(1 - \frac{1 + 0.55(h-1)}{h}\right)$$

$$\phi = \left(0.45\frac{h-1}{h}\right)$$

Now, this derived expression will be used to compute the maximum savings obtained by implementing network coding in the considered regular topologies (ring, star, and line) as the number of nodes increase to infinity in the following subsections.

3.2.1 Star Topology

$$\phi = \left(0.45\frac{\frac{2(N-1)}{N} - 1}{\frac{2(N-1)}{N}}\right) = \left(0.45\frac{N-2}{2(N-1)}\right)$$

$$\lim_{n\to\infty} \phi = \lim_{n\to\infty}\left(0.45\frac{\frac{2(N-1)}{N} - 1}{\frac{2(N-1)}{N}}\right) = 0.225$$

3.2.2 Ring Topology (Odd number of nodes)

$$\phi = \left(0.45\frac{\frac{N+1}{4} - 1}{\frac{N+1}{4}}\right) = \left(0.45\frac{N-3}{N+1}\right)$$

$$\lim_{n\to\infty} \phi = \lim_{n\to\infty}\left(0.45\frac{N-3}{N+1}\right) = 0.45$$

3.2.3 Ring Topology (Even number of nodes)

$$\phi = \left(0.45\frac{\frac{N^2}{4(N-1)} - 1}{\frac{N^2}{4(N-1)}}\right) = \left(0.45\left(\frac{N-2}{N}\right)^2\right)$$

$$\lim_{n\to\infty}\phi = \lim_{n\to\infty}\left(0.45\left(\frac{N-2}{N}\right)^2\right) = 0.45$$

3.2.4 Line Topology

$$\phi = \left(0.45\frac{\frac{N+1}{3}-1}{\frac{N+1}{3}}\right) = \left(0.45\frac{N-2}{N+1}\right)$$

$$\lim_{n\to\infty}\phi = \lim_{n\to\infty}\left(0.45\frac{N-2}{N+1}\right) = 0.45$$

From the analysis above, it has been shown that power savings asymptotically approach 45% and 22.5% for the ring (and line), and star topology respectively. If $r = 1$ which implies that network coding port is as efficient as conventional ports, then the savings increase to 50% and 25% respectively.

4. Conclusion

The design and simulation of adaptive energy saving schemes in IP over Wavelength Division Multiplexing (WDM) networks is presented. Particularly, modification in node architecture to improve energy efficiency (increase energy saving) of IP over WDM networks under unicast conditions is presented. To enhance the energy efficiency on the node architecture, mixed integer linear programming (MILP) technique is used. The architectural and mathematical models to realize energy consumption reduction in IP network-based applications and equipment over WDM networks are also presented. The models included approach to determine the energy per bit consumption of IP and Ethernet i.e. the routers and switches, as well as energy saving models for IP over WDM. Also, adaptive routing scheme using Mixed Integer Linear Programming and network coding partitioning scheme for core communication network via IP over WDM are presented. The essence of all the models are to optimize the energy efficiency in the IP over Wavelength Division Multiplexing (WDM) networking infrastructures. Simulation was conducted in MATLAB for performance evaluation of the models presented in this study and the results demonstrated the effectiveness of the models in reducing the energy consumption in the IP over WDM network.

References

1. Sarangapani, J. (2017). *Wireless ad hoc and sensor networks: protocols, performance, and control*. CRC press.
2. Mirtchev, S. (2015). Internet evolution, teletraffic and QoS: a survey of network traffic. *Electrotechnica & Electronica (E+ E) Journal*, *50*(1-2), 2-17.
3. Zhang, C., Patras, P., & Haddadi, H. (2019). Deep learning in mobile and wireless networking: A survey. *IEEE Communications surveys & tutorials*, *21*(3), 2224-2287.
4. Kolawole, O. Y. (2019). On the performance of hybrid beamforming for millimeter wave wireless networks.
5. Vermesan, O., Eisenhauer, M., Sundmaeker, H., Guillemin, P., Serrano, M., Tragos, E. Z., ... & Bahr, R. (2017). Internet of things cognitive transformation technology research trends and applications. *Cognitive Hyperconnected Digital Transformation: Internet of Things Intelligence Evolution*.
6. Riccardi, E., Gunning, P., de Dios, Ó. G., Quagliotti, M., López, V., & Lord, A. (2018). An operator view on the introduction of white boxes into optical networks. *Journal of Lightwave Technology*, *36*(15), 3062-3072.
7. Winzer, P. J. (2020). Transmission system capacity scaling through space-division multiplexing: a techno-economic perspective. In *Optical Fiber Telecommunications VII* (pp. 337-369). Academic Press.
8. Horvath, T., Munster, P., Oujezsky, V., & Bao, N. H. (2020). Passive optical networks progress: a tutorial. *Electronics*, *9*(7), 1081.
9. Alsharif, M. H., & Nordin, R. (2017). Evolution towards fifth generation (5G) wireless networks: Current trends and challenges in the deployment of millimetre wave, massive MIMO, and small cells. *Telecommunication Systems*, *64*(4), 617-637.
10. Agrell, E., Karlsson, M., Chraplyvy, A. R., Richardson, D. J., Krummrich, P. M., Winzer, P., ... & Gisin, N. (2016). Roadmap of optical communications. *Journal of Optics*, *18*(6), 063002.
11. Winzer, P. J., & Neilson, D. T. (2017). From scaling disparities to integrated parallelism: A decathlon for a decade. *Journal of Lightwave Technology*, *35*(5), 1099-1115.
12. He, J., Norwood, R. A., Brandt-Pearce, M., Djordjevic, I. B., Cvijetic, M., Subramaniam, S., ... & Peyghambarian, N. (2014). A survey on recent advances in optical communications. *Computers & Electrical Engineering*, *40*(1), 216-240.
13. Zou, J. S., Sasu, S. A., Lawin, M., Dochhan, A., Elbers, J. P., & Eiselt, M. (2020). Advanced optical access technologies for next-generation (5G) mobile networks. *Journal of Optical Communications and Networking*, *12*(10), D86-D98.
14. Mendiola, A., Fuentes, V., Matias, J., Astorga, J., Toledo, N., Jacob, E., & Huarte, M. (2016). An architecture for dynamic QoS management at Layer 2 for DOCSIS access networks using OpenFlow. *Computer Networks*, *94*, 112-128.
15. Shove, E., Watson, M., & Spurling, N. (2015). Conceptualizing connections: Energy demand, infrastructures and social practices. *European journal of social theory*, *18*(3), 274-287.
16. Morley, J., Widdicks, K., & Hazas, M. (2018). Digitalisation, energy and data demand: The impact of Internet traffic on overall and peak electricity consumption. *Energy Research & Social Science*, *38*, 128-137.
17. Wu, J., Zhang, Y., Zukerman, M., & Yung, E. K. N. (2015). Energy-efficient base-stations sleep-mode techniques in green cellular networks: A survey. *IEEE communications surveys & tutorials*, *17*(2), 803-826.
18. Miglani, A., Kumar, N., Chamola, V., & Zeadally, S. (2020). Blockchain for Internet of Energy management: Review, solutions, and

challenges. *Computer Communications*, *151*, 395-418.

19. Devine-Wright, P., & Batel, S. (2017). My neighbourhood, my country or my planet? The influence of multiple place attachments and climate change concern on social acceptance of energy infrastructure. *Global Environmental Change*, *47*, 110-120.
20. Van Heddeghem, W., Lambert, S., Lannoo, B., Colle, D., Pickavet, M., & Demeester, P. (2014). Trends in worldwide ICT electricity consumption from 2007 to 2012. *Computer Communications*, *50*, 64-76.
21. Lambert, S., Van Heddeghem, W., Vereecken, W., Lannoo, B., Colle, D., & Pickavet, M. (2012). Worldwide electricity consumption of communication networks. *Optics express*, *20*(26), B513-B524.
22. Malmodin, J., & Lundén, D. (2018). The energy and carbon footprint of the global ICT and E&M sectors 2010–2015. *Sustainability*, *10*(9), 3027.
23. Wahlroos, M., Pärssinen, M., Manner, J., & Syri, S. (2017). Utilizing data center waste heat in district heating–Impacts on energy efficiency and prospects for low-temperature district heating networks. *Energy*, *140*, 1228-1238.
24. Lundén, D., Malmodin, J., Bergmark, P., & Lövehagen, N. (2022). Electricity consumption and operational carbon emissions of European telecom network operators. *Sustainability*, *14*(5), 2637.
25. Nikolova, C., & Gutierrez, T. (2020). Use of microorganisms in the recovery of oil from recalcitrant oil reservoirs: Current state of knowledge, technological advances and future perspectives. *Frontiers in microbiology*, *10*, 2996.
26. Mukhammadsidiqov, M., & Turaev, A. (2020). The Influence Of The Energy Factor On Modern International Relations. *The American Journal of Political Science Law and Criminology*, *2*(12), 5-15.
27. Welsby, D., Price, J., Pye, S., & Ekins, P. (2021). Unextractable fossil fuels in a 1.5 C world. *Nature*, *597*(7875), 230-234.
28. Martins, F., Felgueiras, C., Smitkova, M., & Caetano, N. (2019). Analysis of fossil fuel energy consumption and environmental impacts in European countries. *Energies*, *12*(6), 964.
29. Jin, C., Bai, X., Yang, C., Mao, W., & Xu, X. (2020). A review of power consumption models of servers in data centers. *applied energy*, *265*, 114806.
30. Zhang, Q., Meng, Z., Hong, X., Zhan, Y., Liu, J., Dong, J., ... & Deen, M. J. (2021). A survey on data center cooling systems: Technology, power consumption modeling and control strategy optimization. *Journal of Systems Architecture*, *119*, 102253.
31. Chen, X., Jiang, S., Chen, Y., Zou, Z., Shen, B., Lei, Y., ... & Gou, H. (2022). Energy-saving superconducting power delivery from renewable energy source to a 100-MW-class data center. *Applied Energy*, *310*, 118602.
32. Deymi-Dashtebayaz, M., Namanlo, S. V., & Arabkoohsar, A. (2019). Simultaneous use of air-side and water-side economizers with the air source heat pump in a data center for cooling and heating production. *Applied thermal engineering*, *161*, 114133.
33. Li, H., Hou, J., Hong, T., Ding, Y., & Nord, N. (2021). Energy, economic, and environmental analysis of integration of thermal energy storage into district heating systems using waste heat from data centres. *Energy*, *219*, 119582.